CHAPTER-5

Formulation, optimization and characterization of crosslinked chitosan microspheres

CHAPTER 5

Formulation, optimization and characterization of crosslinked chitosan microspheres

5.1. METHODS

5.1.1. Part A

Screening, optimization and characterization of polyelectrolyte complexed microspheres of chitosan and sodium alginate (CS-Ca-SA)

5.1.1.1. Experimental Design

Plackett-Burman Factorial Design (PBFD) was used to estimate optimum critical independent fabrication variables affecting desirable characteristics of microspheres. The seven critical independent fabrication variables selected at low (-) and high (+) levels based on extensive literature survey. The selected fabrication variables included sodium alginate concentration (SA), chitosan concentration (CS), calcium carbonate concentration (CaC), surfactant concentration (SC), crosslinking time (CT), agitation speed (AS), and aqueous : oil phase ratio (PR) as depicted in Table 5.1. Particle size (PS), entrapment efficiency (EE), burst release (B) calculated by drug released within 12 h and time for attaining 80% cumulative drug release ($T_{80\%}$) were selected as desirable dependent responses. Pareto and regression analysis was performed on the data obtained to evaluate the correlations between various selected dependent and independent variables using following linear equations:

$$Y = A_0 + A_1\,CS + A_2\,SA + A_3 CaC + A_4 SC + A_5 CT + A_6 AS + A_7 PR$$

Where Y is the selected response, A_0 is the constant value and A_1, A_2, A_3, A_4, A_5, A_6, A_7 are coefficients of respective factors. An analysis of variance (ANOVA) was performed at 95% confidence interval to test the significance ($p\text{-}value < 0.05$) of all coefficients and eliminate the less significant terms. Optimization of microspheres

was performed by response optimizer tool of Minitab® 17. The validation of generated model and optimized batch was done by comparing the magnitudes of predicted and experimental values of the responses using percent bias as follows.

Bias = [(predicted value - experimental value)/predicted value] x100

Table 5.1: Independent fabrication variables and dependent response variables associated with CS-Ca-SA microsphere formulation.

Independent fabrication variables	**Low (-) level**	**High (+) level**
Concentration of sodium alginate (SA) (% w/v)	2	5
Concentration of chitosan (CS) (% w/v)	2	4
Concentration of calcium carbonate (CaC) (% w/v)	2.5	5
Crosslinking time (CT) (min)	30	60
Agitation speed (AS) (rpm)	500	2000
Surfactant concentration (SC) (% w/v)	0.5	1
Phase ratio (aqueous : oil) (PR)	1:2	1:6
Dependent response variables	**Constraints**	
Particle Size (PS) (μm)	Minimize	
Entrapment efficiency for ornidazole (EEOZ) (%)	Maximize	
Entrapment efficiency for doxycycline hyclate (EEDX) (%)	Maximize	
Burst release of ornidazole (BOZ) (%)	Minimize	
Burst release of doxycycline hyclate (BDX) (%)	Minimize	
Time for 80% cumulative drug release (TOZ) (%)	Maximize	
Time for 80% cumulative drug release (TDX) (%)	Maximize	

5.1.1.2. Formulation of microspheres

CS-Ca-SA microspheres were formulated by combination of w/o emulsion-internal ionic gelation technique followed by polyelectrolyte complexation with little modifications (Fig 5.1) (Poncelet *et al.,* 1992; Zhang *et al.,* 2011). Briefly, SA solution was prepared into preheated (60 °C) Millipore water on mechanical shaker. Drugs (OZ + DX) solution was prepared on bath sonicator such that final

concentration of 25% and 10% (w/w of polymer) was obtained and mixed with SA solution with agitation. This SA-drug aqueous mixture was dispersed into paraffin oil containing anhydrous $CaCO_3$ and Tween 80: span 80 (1:1) under agitation. Agitation was continued for one hour to stabilize w/o emulsion and solidification of droplets. After specified time, calcium carbonate was dissolved by adding 10 ml of liquid paraffin containing glacial acetic acid (1% v/v). It was then kept on agitation for 60 min to allow complete dissolution of $CaCO_3$.

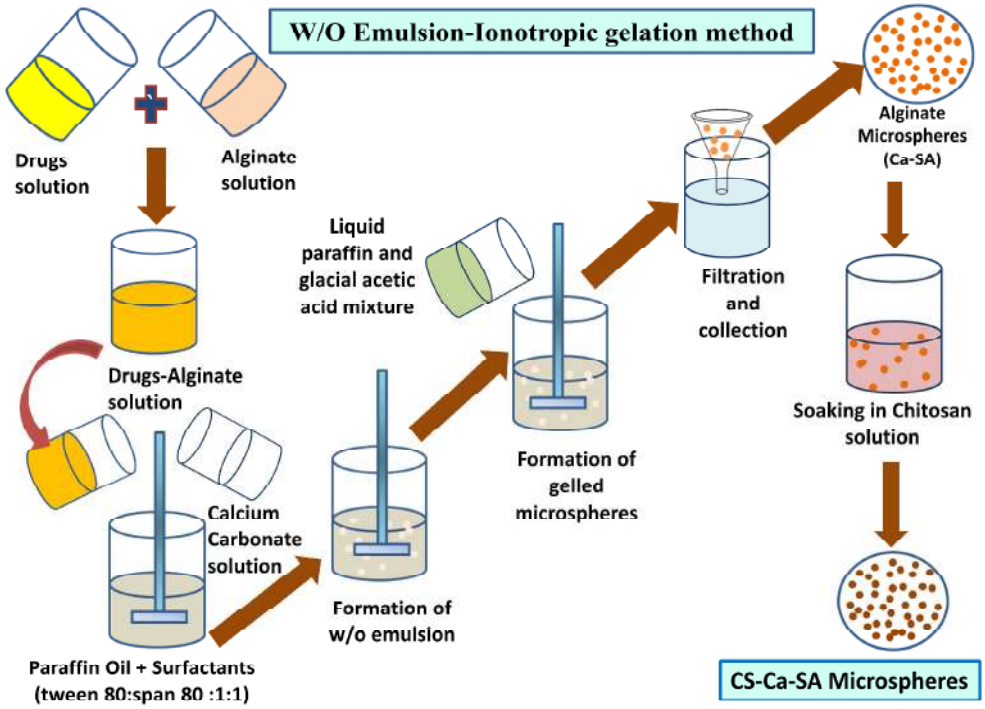

Figure 5.1: Schematic representation of w/o emulsion crosslinking method for the formulation of chitosan-alginate (CS-Ca-SA) polyelectrolyte complexed microspheres.

After 12 h of agitation the formed gelled microspheres were collected by filtration followed by subsequent 5-6 washings with n-hexane and acetate buffer pH 5.5 to remove paraffin oil and excess of calcium/chitosan respectively. Final washings were done with Millipore water. Confirmations regarding removal or absence of oily phase were done by optical microscope (Dwinter optical Inc., India). Microspheres collected at this stage were designated as alginate (Ca-SA) microspheres. At second

stage, polyelectrolyte complexes *viz.* chitosan-alginate (CS-Ca-SA) microspheres were formed by immersing the alginate microspheres into chitosan solution maintained at pH 6.5 for specified time (regarded as CT) under mild agitation at 50 rpm (Ribeiro *et al.,* 2005). The particles were finally filtered, washed with 1% w/v acetic acid solution and Millipore water (to remove non-crosslinked chitosan) and oven dried. Placebo CS-Ca-SA microspheres were also formulated without drug.

5.1.1.3. Dependent response variables

5.1.1.3.1. *Particle size (PS)*

PS of microspheres was determined using optical microscope equipped with Dwinter Biowizard 4.1 software. The eyepiece micrometer was calibrated with the help of stage micrometer. The diameter of 100 microspheres was measured randomly (Bai *et al.,* 2004). The PS was calculated using following Edmondson's Equation.

$$PS = \frac{\sum number\ of\ microspheres\ in\ a\ size\ range\ X\ mean\ size\ in\ that\ range}{\sum number\ of\ microspheres\ in\ a\ size\ range}$$

5.1.1.3.2. *Entrapment Efficiency (EE)*

50 mg of microspheres were soaked in 10 ml of PBS pH 6.8 and bath sonicated for 30 min, and then centrifuged at 6000 rpm and filtered. Free drug content was calculated from filtrate using simultaneous equation UV method as mentioned in chapter 4. The % EE of drugs was determined using following equation;

$$EE\ (\%) = \frac{Total\ amount\ of\ drug\ added - free\ drug\ content}{Total\ amount\ of\ drug\ added} \times 100$$

5.1.1.3.3. *In-vitro drug release parameters*

For *in-vitro* drug release study of periodontal medicines, McIlvaine buffer pH 6.8 has frequently been used as release media. However, interactions between tetracyclines and chitosan with citric acid were observed (Hejazi and Amiji, 2002). Therefore, *in-vitro* drug release was carried out in PBS pH 6.8 using the dialysis bag technique (Bansal *et al.,* 2009; Jha *et al.,* 2011). Dialysis bags (12,000-14,000 Dalton,

Himedia labs, India) containing suspension of microspheres (100 mg) in 5 ml of PBS pH 6.8 were tightened at the end of paddle of dissolution apparatus (Campbell Electronics, India) filled with 500 ml of same buffer maintained at 37±0.5 °C and stirred at 50 rpm. At predefined time intervals (0, 2, 4, 8, 12, 24, 48, 72, 96, 120 h), 5 ml of samples were withdrawn from the release medium and replenished with equivalent volume of fresh dissolution medium to maintain sink condition. Collected samples were filtered using 0.45 µ membrane filters and drug release was estimated by UV method as mentioned in chapter 4. Time for 80% drug release ($T_{80\%}$) and burst release (BOZ and BDX) was calculated from % cumulative drug release *vs.* time plots using MS excel 2010 and Origin Pro 5 software.

5.1.1.4. Evaluation of optimized formulation

5.1.1.4.1. Process yield

Process yield (PY) of formulated microspheres were determined from the percentage ratio of total amount of microspheres recovered after drying to the total amount of solid content (drugs + polymer + crosslinking agent) used for the formation of microspheres. It is calculated in percentage as follows:

$$PY\ (\%) = \frac{Total\ amount\ of\ microspheres\ recovered}{Total\ amount\ of solid\ content\ added} \times 100$$

5.1.1.4.2. Drug release kinetics and diffusion coefficient

The release profiles were fitted on various kinetic models of release including Zero-order, First-order, Higuchi, Hixson-Crowell and Korsmeyer-Peppas model to determine drug release mechanism by using Microsoft excel office 2010.

$$\frac{M_t}{M_\infty} = kt \qquad \text{(Zero-order equation)}$$

$$ln\left(1 - \frac{M_t}{M_\infty}\right) = -kt \qquad \text{(First-order equation)}$$

$$\frac{M_t}{M_\infty} = kt^{1/2} \qquad \text{(Higuchi equation)}$$

$$\left(1-\frac{M_t}{M_\infty}\right)^{1/3} = -kt \qquad \text{(Hixson-Crowell equation)}$$

$$\frac{M_t}{M_\infty} = kt^n \qquad \text{(Korsmeyer-Peppas equation)}$$

where M_t/M_∞, is the fraction of drug released at any time 't', 'k' is release constant dependent on structure and composition of drug/polymer system, and 'n' is the release exponent, determines mechanism of drug release. For spherical particles, when $n \leq 0.43$, the drug is released from the polymer with Fickian diffusion mechanism. If $0.43 < n < 0.85$, it indicates non-Fickian with both diffusion and swelling controlled drug release (anomalous transport) mechanism, whereas if $n = 0.85$, zero-order drug release is followed. Values $n > 0.85$ indicates case-II transport related to polymer relaxation due to swelling (Dai *et al.,* 2008).

Furthermore, the diffusion constant 'D' was determined using fractional release of drugs (Mt/M_∞) as a function of release time 't' from following equations;

$$\frac{M_t}{M_\infty} = \sqrt{\frac{16Dt}{\pi r^2}}$$

$$D = \frac{1}{4} m\pi r$$

Where m is the slope of curve (M_t/M_∞ *vs* $t^{-1/2}$), r is the average diameter of microspheres and 'π' is a constant with value of 3.14 (Gupta and Jabrail, 2007).

5.1.1.4.3. Solid state characterizations

5.1.1.4.3.1. Morphology

The detailed shape, size and structure of microspheres were observed by scanning electron microscope (SEM) (FEI, Quanta 200F, Japan) attached to Image J software. Furthermore, the elemental composition of microspheres was estimated by using Energy-dispersive X-ray analysis (EDXA) attachment to SEM. It was performed at an acceleration voltage of 20 kV and magnification of 2000X.

5.1.1.4.3.2. Fourier-Transform Infrared spectroscopy (FTIR)

FTIR studies of drugs, polymers and microspheres were done to identify and analyze any possible interaction between them by using Shimadzu, Model 8400, Japan. The samples were prepared by pressed pellet technique using potassium bromide. Samples were scanned from 4000 to 400 cm^{-1} with a resolution of 4 cm^{-1} for 20 scans.

5.1.1.4.3.3. Differential scanning calorimetry (DSC)

DSC thermograms of drugs, polymers and microspheres were plotted using Mettler DSC 25, India. Samples equivalent to 5 mg were placed in aluminium pan and hermetically sealed and heated at a rate of 10° C/min, covering temperature range of 0-300 °C under flow of nitrogen atmosphere at the rate of 60 ml/min.

5.1.1.4.3.4. X-ray diffraction (XRD)

XRD patterns of drugs, polymers and microspheres were obtained on portable X-ray diffractometer (Rigaku, Japan) to characterize alterations in crystallinity of samples. The diffraction patterns were recorded using Ni-filtered Cu-Kα radiation operated at a voltage of 40 kV and 20 mA. Diffraction patterns were obtained by varying diffraction angle (2θ) at 0-60º at a scanning rate of 1º/s.

5.1.1.4.4. Swelling and erosion studies

The swelling abilities of microspheres were estimated by soaking about 50 mg of microspheres into 5 ml of simulated saliva (pH 6.8) contained in glass vials kept in a beaker containing water maintained at 37 °C for 24 h (Marques *et al.,* 2011). The swollen microspheres were weighed after blotting with filter paper to remove surface water. The percentage swelling (S) was expressed as follows;

$$S\,(\%) = \frac{W_t - W_0}{W_0} \times 100$$

Where W_t refers to the final weight of microspheres after swelling and W_0 refers to initial weight of microspheres taken (Xu *et al.,* 2007).

At predetermined time intervals, the hydrated microspheres were carefully taken from vials and blotted with tissue paper. Then, the microspheres were dried at 40 °C until constant weight. After drying the samples were weighed to determine remaining dry weight (W_d) (Govender *et al.,* 2005; Sriamornsak *et al.,* 2007). The erosion was estimated in terms of % remaining weight as follows:

$$\%\ Remaining\ weight = \left(1 - \frac{W_0 - W_d}{W_0}\right) 100$$

5.1.1.4.5. Surface pH

For surface pH determination, about two mg of microspheres were allowed to swell in 1 ml of PBS pH 6.8 placed in glass test tubes for 5 min (Govender *et al.,* 2005). The surface pH was recorded by bringing the glass microelectrode of the Deluxe pH meter (Perfit, India) on the surface of microspheres after allowing it to equilibrate for one minute.

5.1.1.4.6. *In-vitro* mucoadhesion

In-vitro mucoadhesion was calculated in terms of weight percentage of microspheres that remain adhered to the mucosal surface with minor modifications in the method reported by Jha *et al.,* (2011) (Jha *et al.,* 2011). In brief, specified weighed quantity of microspheres (W_0) was spread on cleaned and cut ($1 \times 1\ cm^2$) bovine cheek pouch to simulate mucosal membranes of periodontal cavity. The cheek pouch membrane was fixed on a glass plate with the help of cyanoacrylate adhesive. The microspheres were kept for 10 min for proper hydration and adhesion. Afterwards the glass plate was made to incline at an angle of 45° with the help of stand and pouch membrane was washed with PBS (pH 6.8). The washings were collected and oven dried (40 °C) to determine non-adhered microspheres (W_n). Mucoadhesion (%M) was estimated by the following formula;

$$\%\ M = \frac{W_0 - W_n}{W_0} \times 100$$

5.1.1.4.7. Cytocompatibility study

Sulphorhodamine B (SRB) assay method has been previously reported for the assessment of biocompatibility of endodontic filling material Resilon on L929 cell lines (Economides *et al.,* 2008). Unlike, 3-(4,5-dimethylthiazol-2-yl)-2,5-diphenyltetrazolium bromide (MTT) assay, SRB gives protein content of cells that is linear over a cell density range. Therefore, it is more preferred cytotoxicity assay based on its sensitive, simple, linear, reproducible, stable end point and more rapid results than MTT (Houghton *et al.,* 2007).

Mouse skin fibroblasts cell lines (L929) were cultured in complete medium comprising of Dulbecco's modified Eagle's medium (DMEM), 10% fetal bovine serum and 100 µg/mL streptomycin and 100 IU/mL penicillin as antibiotics. The cells were preserved at 37ºC in a humidified atmosphere with 5% CO_2 and were subcultured twice a week.

The extracts from optimized batch were prepared by incubating microspheres at concentrations of 0.01 g/ml (A), 0.05 g/ml (B), and 0.1 g/ml (C) in DMEM culture medium for 24 h at 37 °C. The extracts were filtered *via.* 0.22 µm membrane filter and stored at 20 °C. 100 µl of filtered, sterile extracts were added to L929 cells contained in 96 well microplates and incubated for 120 h (n = 6). Control wells were treated with 100 µL DMEM. At the established time points, cell numbers were estimated by means of the SRB assay.

Further, the culture medium was aspirated and 100 µL of 10% cold (4 °C) trichloroacetic acid (TCA) were added gently to the wells for fixation. Microplates were left for 30 min at 4 °C, washed five times with millipore water and dried at room temperature for 24 h. Subsequently, 100 µL 0.4% (w/v) SRB in 1% acetic acid solution were added to each well and kept at room temperature for 20 min. The unbound SRB was removed by washing five times with 1% acetic acid. Protein bound SRB was dissolved in 200 µL 10 mM unbuffered trisbase (Tris hydroxyl methyl aminomethane) solution. Optical density was read at 540 nm by subtracting the

background measurement of 690 nm using micro plate reader (Bio-rad, ELISA plate reader). The percentage cell viability and growth inhibition was calculated by following equation;

$$\%\, Cell\ viability = \frac{OD_{control} - OD_{test}}{OD_{control}} \times 100$$

$$\%\, Cell\ growth\ inhibition = 1 - \%\, cell\ viability$$

Concentration *vs.* % inhibitions curves were plotted and $IC_{50\%}$ (Concentration for 50% cell growth inhibition) values were estimated by regression analysis. Moreover, the cells were treated with microspheres at concentrations A (0.01 g/ml), B (0.05 g/ml) and C (0.1 g/ml), respectively for 24 h. After incubation period the cells were taken out from the cell culture, rinsed with PBS pH 6.8 and stained with fluorescein diacetate (FDA) and ethidium bromide (EDB) then evaluated microscopically using confocal laser scanning microscope (Carl Zeiss, Oberkochen, Germany).

5.1.1.4.8. Antimicrobial activity study

For estimating antimicrobial activity, samples containing released drug obtained during *in-vitro* drug release study were assessed for zone of inhibition by disc diffusion method. Drug release samples collected at selected time intervals (12, 24, 48, 72 h) were tested for antimicrobial activity for *Staphylococcus aureus* (MTCC96) and *Escherichia coli* (MTCC723). Briefly, 15 ml of molten Muller-Hinton agar media (Himedia labs, India) was poured into sterilized petri-plates (90 mm*15 mm) and allowed to solidify. One ml of cultured bacteria adjusted to 0.5 McFarland standards in sterile saline to achieve concentration of 10^7 ml^{-1} colony forming units (CFU) was swabbed on petri-plates using sterile swab sticks. Then, 10 µl of released drug samples were poured on sterile disc (6X6 mm) placed on the surface of media and incubated for 24 h at 37±0.5 °C. The diameter (mm) of zone of bacterial growth inhibition was calculated by subtracting disc diameter from total zone of inhibition.

5.1.1.4.9. Stability study

The stability studies of optimized batch of microspheres was performed following ICH guidelines- Q1A (R2) *Stability Testing of New Drug Substances and Products*. For stability studies, the optimized batch of microspheres were packed in high density plastic bottles and stored at three storage conditions 5±3 °C, 40±2 °C, 75±5% and 25 °C, 70% RH by keeping in refrigerator, humidity controlled oven (High Temperature) and room temperature, respectively for six months. The microspheres were investigated for morphology, PS, EE and total drug content (TDC) to assess the stability. The shelf-life of microspheres were evaluated using Minitab® software *ver.* 17.

5.1.2. Part B

Design, optimization and characterization of chitosan-Tripolyphosphate (CSTPP) microspheres

5.1.2.1. Formulation of CSTPP microspheres

5.1.2.1.1. Method A (Ionic-gelation crosslinking)

In this method, microspheres were prepared by the ionic crosslinking of CS and TPP by directly injecting TPP into CS solution (Li *et al.,* 2008b) (Fig 5.2). Briefly, CS solution was prepared in 1% v/v acetic acid by filtering *via.* nylon cloth to remove undissolved polymer. Both drugs were solubilized in 5 ml of millipore water and mixed with CS homogeneously on bath sonicator. Then, 25 ml of TPP solution was added drop-wise with the help of 22 G needle into 50 ml of CS-drug solution under continuous agitation. Colloidal microspheres were formed spontaneously and were hardened by keeping for extensive crosslinking under agitation for the stated crosslinking time (CT). The microspheres were filtered, washed and collected. The obtained microspheres were freeze-dried (-45 °C and 0.08 mbar) (FD) by redispersion in water or oven-dried (OD) (40 °C) and stored in desiccators.

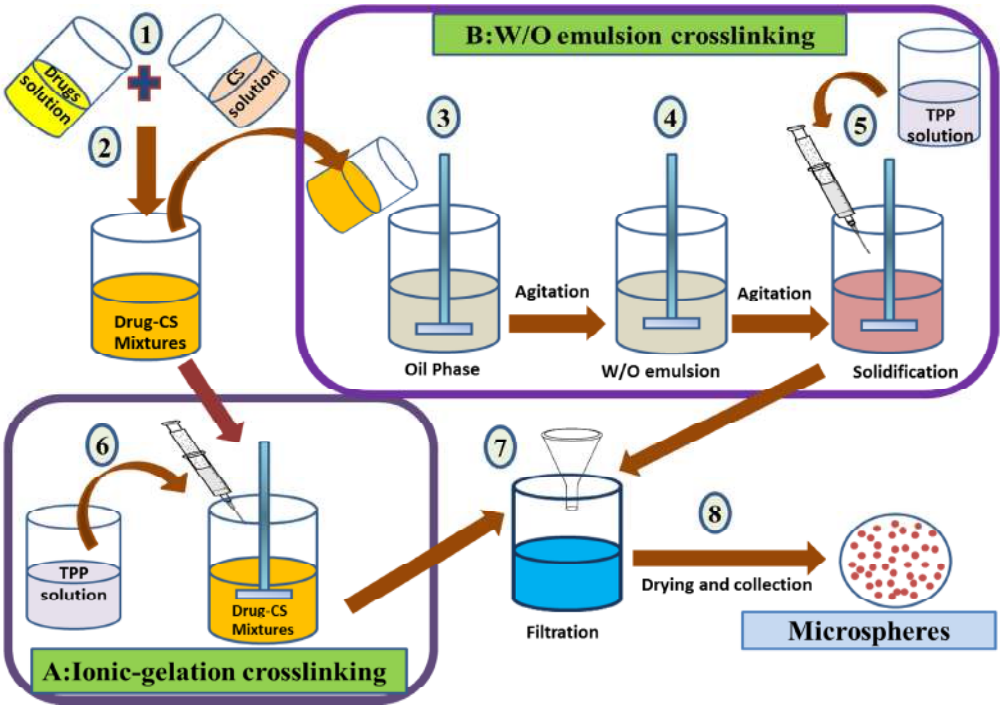

Figure 5.2: Diagrammatic illustration of ionic-gelation crosslinking (Method A) and w/o emulsion crosslinking method (Method B) for preparation of microspheres. ① Dissolution of drugs and polymers in respective solvents (Method A and B); ② Mixing of drug solution and polymer (Method A and B); ③ Dropping of drug-polymer solution to liquid paraffin (Method B); ④ Formation of stable w/o emulsion (Method B); ⑤ Dropping of crosslinking agent to solidify the formed aqueous droplets in w/o emulsion with the help of syringe (Method B); ⑥ Addition of crosslinking agent directly to the drug-polymer solution (Method A); ⑦ Filtration and washing (Method A and B); ⑧ Drying and collection of microspheres (Method A and B).

5.1.2.1.2. Method B (w/o emulsion crosslinking method)

CS, drug and TPP solution were prepared in similar way as discussed in method A (Fig. 5.2). Homogeneously mixed drug and CS solution was then added to 100 ml of light liquid paraffin oil containing 0.5% w/v span 80: tween 80 mixture (1:1) to form w/o emulsion under agitation for 10 min to stabilize emulsion (Anal *et al.,* 2006). Then, TPP solution was dropped slowly using 22G needle to the formed w/o emulsion causing spontaneous crosslinking of aqueous droplets. The formed droplets were further hardened and crosslinked by keeping on agitation for the stated time. The formed microspheres were separated by filtration and washed with

petroleum ether (40-60 °C) and water to remove traces of paraffin and TPP respectively. The microspheres were then either FD or OD and stored in desiccator.

Table 5.2. Independent and dependent variables associated with CSTPP microsphere formulation.

Independent fabrication variables	**Low (-) level**	**High (+) level**
Method of preparation (MOP)	A	B
Concentration of chitosan (CS) (% w/v)	0.5	3
Concentration of tripolyphosphate (TPP) (% w/v)	1	5
Crosslinking time (CT) (Minutes)	30	120
Agitation speed (AS) (rpm)	1000	2000
Drying technique (DT)	Freeze-dried (FD)	Oven-dried (OD)
Dependent variables	**Constraints**	
Process yield (PY) (% w/w)	Maximize	
Particle size **(**PS) (μm)	Minimize	
EE of drugs (EEOZ and EEDX) (%)	Maximize	
Cumulative burst release of drugs (BOZ and BDX) (%)	Minimize	
$T_{80\%}$ cumulative release of drugs (TOZ and TDX) (h)	Maximize	

5.1.2.2. Experimental Design

PBFD was used to estimate the correlations between independent variables and selected dependent variables or responses as shown in Table 5.2. Six independent variables such as; method of preparation of microspheres (MOP), concentration of chitosan (CS), tripolyphosphate (TPP), crosslinking time (CT), agitation speed (AS) and drying technique (DT) were studied at two levels “low” and “high” selected on the basis of preliminary trial studies and literature survey. Process yield (PY), particle size (PS), encapsulation efficiency (EE), burst release and slow release (measured by $T_{80\%}$) of drugs were chosen as responses. The statistical analysis and optimization of batches was done as discussed in *sub-section 5.1.1.1.*

5.1.2.3. Dependent response variables

5.1.2.3.1. Process yield

PY was calculated following procedure as mentioned in *sub-section 5.1.1.4.1.*

5.1.2.3.2. Particle size

PS was calculated following procedure as mentioned in *sub-section 5.1.1.3.1.*

5.1.2.3.3. Encapsulation Efficiency (EE)

EE was calculated following procedure as mentioned in *sub-section 5.1.1.3.2.*

5.1.2.3.4. *In-vitro* drug release parameters

Same procedure was followed as mentioned in *sub-section 5.1.1.3.3.*

5.1.2.4. Characterization of optimized formulation

5.1.2.4.1. Drug release kinetics

Same procedure was followed as mentioned in *sub-section 5.1.1.4.2.*

5.1.2.4.2. Solid state characterization

5.1.2.4.2.1. Morphology

Same procedure was followed as mentioned in *sub-section 5.1.1.4.3.1*

5.1.2.4.2.2. Fourier Transform Infrared Spectroscopy

Same procedure was followed as mentioned in *sub-section 5.1.1.4.3.2.*

5.1.2.4.2.3. Differential Scanning Calorimetry

Same procedure was followed as mentioned in *sub-section 5.1.1.4.3.*3

5.1.2.4.2.4. X-ray Diffraction

Same procedure was followed as mentioned in *sub-section 5.1.1.4.3.4*

5.1.2.4.3. Swelling and erosion studies

Same procedure was followed as mentioned in *sub-section 5.1.1.4.4.*

5.1.2.4.4. Surface pH

Same procedure was followed as mentioned in *sub-section 5.1.1.4.5*

5.1.2.4.5. *In-vitro* mucoadhesion

Same procedure was followed as mentioned in *sub-section 5.1.1.4.6.*

5.1.2.4.6. Cytocompatibility study

Same procedure of SRB assay was followed as mentioned in *sub-section 5.1.1.4.7.*

5.1.2.4.7. Antimicrobial activity

Same procedure was followed as mentioned in *sub-section 5.1.1.4.8.*

5.1.2.4.8. Stability study

Same procedure was followed as mentioned in *sub-section 5.1.1.4.9.*

5.1.3. Part C

Optimization and characterization of chitosan - vanillin (CSV) microspheres using dual design approach

5.1.3.1. Primary screening of significant formulation variables for crosslinked chitosan microspheres encapsulated with DX using PBFD

5.1.3.1.1. Experimental Design

Design of experiments was performed using PBFD to screen optimum critical fabrication variables affecting desirable characteristics of microspheres using Minitab® *ver.* 17. Eight independent formulation variables and three dependent response variables utilized for the development of crosslinked chitosan microspheres (Table 5.3). Statistical analysis, optimization and validation of batch were done as per standard protocol as mentioned in previous *sub-section 5.1.1.1.*

Table 5.3: Formulation design of CS crosslinked microspheres.

Independent formulation variables	**Low (-) level**	**High (+) level**
Chitosan concentration (CS) (%w/v)	2	4
Type of crosslinker (TCL)	Glutaraldehyde (GLU)	Vanillin (VAN)
Crosslinker Concentration (CLC) (%w/v)	2	6
Crosslinking time (CT) (min)	30	120
Agitation speed (AS) (rpm)	1000	2000
Surfactant concentration (SC) (%w/v)	0.5	2.5
Phase ratio (aqueous : oil) (PR)	1:2	1:6
Oil phase (OP)	Soyabean oil	Liquid paraffin
Dependent response variable	**Target**	
Particle Size (PS) (μm)	Minimize	
Entrapment efficiency (EE) (%)	Maximize	
Time for 80% of cumulative drug release ($T_{80\%}$)	Maximize	

5.1.3.1.2. Formulation of crosslinked microspheres

The CS crosslinked microspheres were formulated by w/o emulsion crosslinking method (Zou *et al.,* 2015) (Fig. 5.3). A predetermined quantity of CS was dissolved in 100 ml of 1% v/v solution of acetic acid following continuous agitation on a magnetic stirrer for one hour (Table 5.3). Weighed quantity of DX was added to CS solution and the mixture was further dropped into oil phase containing mixture of span 80 and tween 80 (1:1) stirred for 15 min. The formed emulsion droplets were crosslinked and solidified to form microspheres by dropping the crosslinker solution under continuous stirring for specified crosslinking time (CT). Towards the end, the fabricated microspheres were filtered, collected and completely washed with petroleum ether (40-60 °C) and dimethyl carbinol to remove liquid paraffin and acetone respectively. The microspheres were freeze dried and stored in desiccators for further characterizations. Based on the chosen crosslinker type the microspheres were

designated as CSV and CSG for VAN, and glutaraldehyde (GLU) crosslinked microspheres respectively.

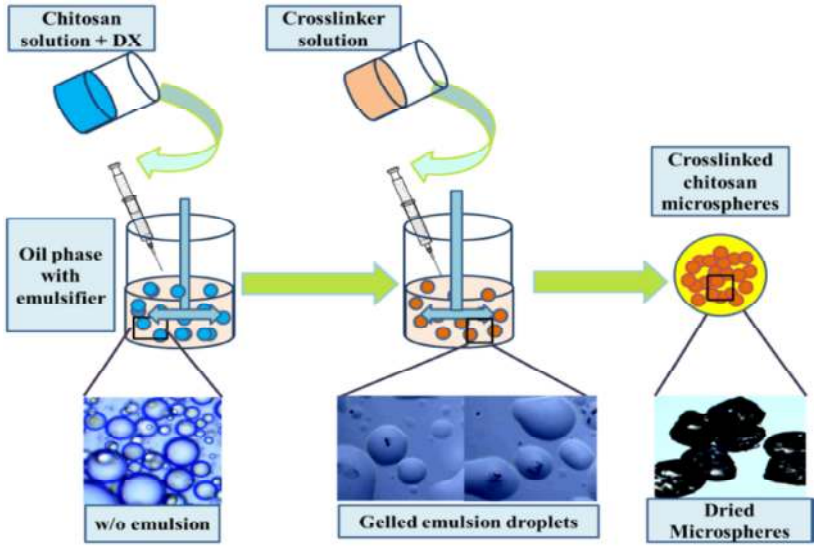

Figure 5.3: Diagrammatic and optical microscopic illustration of steps involved in the formation of chitosan crosslinked microspheres.

5.1.3.1.3. Dependent response variables

5.1.3.1.3.1. Particle size (PS)

Same procedure was followed as mentioned in *sub-section 5.1.1.3.1.*

5.1.3.1.3.2. Entrapment efficiency (%EE)

Same procedure was followed as mentioned in *sub-section 5.1.1.3.2.*

5.1.3.1.3.3. Time for 80% cumulative drug release ($T_{80\%}$)

Same procedure as mentioned in *sub-section 5.1.1.3.3* with some modifications was followed. The release samples were collected at 0, 0.5, 1, 2, 3, 4, 5, 6, 7, 8, 10, 11, 12 days interval and evaluated for drug release parameters.

5.1.3.1.4. Evaluation of optimized formulation

5.1.3.1.4.1. Drug release kinetics

Same procedure was followed as mentioned in *sub-section 5.1.1.4.2*

5.1.3.1.4.2. Solid state characterization

Proton Nuclear Magnetic Resonance (^{1}H NMR) spectrum was obtained using Jeol AL300 FT-NMR, Japan. The samples of chitosan, VAN and CSV microspheres were dissolved in excess of DMSO then placed in 5 mm, 7" NMR tubes and analyzed at 70ºC. Spectroscopy was carried out in the pulsed FT mode at a 300 MHz resonance frequency for protons with 64 scans. Chemical shift are reported in parts per million units relative to Tetramethylsilane (TMS) used as internal standard.

Other solid state characteristics such as, FTIR, DSC, XRD, morphology and EDXA were evaluated as per the procedure mentioned in *sub-section 5.1.1.4.3.*

5.1.3.1.4.3. Swelling studies

Same procedure was followed as mentioned in *sub-section 5.1.1.4.4.*

5.1.3.1.4.4. Degree of crosslinking

Ninhydrin assay was performed to determine the percentage of free amino groups in crosslinked chitosan microspheres (Yuan *et al.,* 2007). The degree of crosslinking was inversely related to free amino groups. 10 mg of microspheres were placed in test-tubes, and 1 ml of Ninhydrin solution (Sigma-Aldrich, India) was added. The solution was boiled for about 10 min and cooled to room temperature. Then, one ml of 95% ethanol was added as stabilizing solvent. The optical density of the sample was determined at 570 nm using a colorimeter. The concentration of amino acid was calculated using D-glucosamine (Sigma-Aldrich, India) as standard.

5.1.3.1.4.5. In-vitro Mucoadhesion

In-vitro mucoadhesion study was done by the method reported by Jha et al. (2011) (Jha *et al.,* 2011) as mentioned in *sub-section 5.1.1.4.6.*

5.1.3.1.4.6. Cytocompatibility study

Same procedure was followed as mentioned in *sub-section 5.1.1.4.7.*

5.1.3.1.4.7. Antimicrobial Study

Same procedure was followed as mentioned in *sub-section 5.1.1.4.8* with some changes. The release samples were collected at 1st and 7th day of release for antimicrobial activity estimation.

5.1.3.1.4.8. Stability studies

Same procedure was followed as mentioned in *sub-section 5.1.1.4.9.*

5.1.3.2. Final optimization of chitosan-vanillin crosslinked (CS-VAN) microspheres based on significant formulation variables using Box-Behnken Experimental Design (BBED)

5.1.3.2.1. Box-Behnken Experimental Design

A response surface methodology, 3 level, 3 factor BBED was specifically selected for its requirements of minimal experimental runs (Table 5.4).

Table 5.4: Box-Behnken Experimental Design for the formulation of chitosan-vanillin crosslinked microspheres.

Independent fabrication variables	**Low level (-)**	**Medium level (0)**	**High level (+)**
A: Concentration of chitosan (CS) (%)	2	3	4
B: Concentration of vanillin (VC) (%)	2	4	6
C: Surfactant concentration (SC) (%)	0.5	1.5	2.5
Dependent response variables	**Unit**		**Target**
Particle size (PS)	µm		Minimize
Entrapment efficiency of OZ (EEOZ)	%		Maximize
Entrapment efficiency of DX (EEDX)	%		Maximize
Time for cumulative 80% OZ release (TOZ)	Days		Maximize
Time for cumulative 80% DX release (TDX)	Days		Maximize
Mucoadhesion (%M)	%		Maximize

BBED was employed to statistically finally optimize the processing factors of microspheres using Design-Expert software® (8.0.6.1, Stat-Ease Inc., US). Chitosan concentration (CS) (%w/v), vanillin (VAN) concentration (VC) (%w/v), and surfactant concentration (SC) (%w/v) were selected as critical independent fabrication variables for microsphere formulation based on preliminary screening using PBFD as mentioned in *sub-section 5.1.3.1.* A total of 15 experiments (excluding two outlier points) was performed to estimate the full model. Polynomial equations were used to study the relationships between independent and dependent response variables along with statistical analysis are illustrated as follows:

$$Y = B_0+B_1CS+B_2VC+B_3SC+B_4CS*VC+B_5CS*SC+B_6VC*SC+B_7CS^2+B_8VC^2+B_9SC^2$$

Y = response, B_0 = constant, B_1, B_2, B_3 = linear coefficients, B_4, B_5 and B_6 = interaction coefficients, B_7, B_8 and B_9 = quadratic coefficients. The optimization and statistical validation of the generated model were established by assessment of statistical parameters such as *p-value* and correlation coefficient (R^2) generated by ANOVA. The optimum values of both dependent and fabrication variables were determined by using graphical optimization tool of Design-Expert software® based on set constrained criterion of desirability. The reliability of developed mathematical models was validated by comparing experimental and predicted responses using % bias.

5.1.3.2.2. Formulation of microspheres

The chitosan-vanillin (CS-VAN) crosslinked microspheres were formulated by w/o emulsion crosslinking method (Zou *et al.,* 2015) using BBED (Table 5.4). Briefly, weighed amount of CS was solubilized in 1% v/v solution of acetic acid and agitated on a magnetic stirrer for one hour (Fig. 5.3). Weighed amounts of drugs were added to CS solution. The obtained drugs and CS solution was then, added to soyabean oil containing surfactant mixture (span 80 and tween 80 at the ratio of 1:1) in a drop-wise manner under continuous agitation of 2000 rpm for 15 min to form stable w/o emulsion. Further, crosslinking of aqueous droplets were accomplished by addition of

VAN solution (in acetone) for two hour. The fabricated microspheres were filtered, collected and completely washed with petroleum ether (40-60 °C) and dimethyl carbinol to remove oil phase and acetone respectively. The microspheres were lyophilized and stored in desiccators for further evaluation.

5.1.3.2.3. Dependent response variables

5.1.3.2.3.1. Particle size

Same procedure was followed as mentioned in *sub-section 5.1.1.3.1.*

5.1.3.2.3.2. Entrapment efficiency

Same procedure was followed as mentioned in *sub-section 5.1.1.3.2.*

5.1.3.2.3.3. Time for 80% drug release ($T_{80\%}$)

Same procedure was followed as mentioned in *sub-section 5.1.3.1.3.3.*

5.1.3.2.3.4. Percent in-vitro mucoadhesion (%M)

Same procedure was followed as mentioned in *sub-section 5.1.1.4.6.*

5.1.3.2.4. *Statistical analysis*

All the experiments were performed in triplicate ($n = 3$) and results are expressed as mean±SD. The results of stability studies were statistically compared with fresh sample by one-way ANOVA followed by Dunnet Multiple comparison test at 95% confidence interval using GraphPad Prism software (version 5.03, US). For cytocompatibility ($n = 6$) and antimicrobial studies all groups were compared with control using two-way ANOVA followed by Bonferroni post-tests and results are reported as mean±standard error mean (SEM). $p < 0.05$ was considered as level of significance.

5.2. RESULTS AND DISCUSSION

5.2.1. Part A

5.2.1.1. w/o internal gelation-polyelectrolyte complexation method

Ca-SA microspheres can be produced by external or internal gelation techniques. The prime difference between both techniques depends on selection of source of calcium ions *i.e.* water soluble salt ($CaCl_2$) for external gelation and water insoluble salt ($CaCO_3$) for internal gelation. In external gelation process, microspheres were formed spontaneously after injecting alginate solution into calcium salt solution. On contrary, in internal gelation method first droplets were emulsified into microemulsion (w/o) by dropping in oil phase. Subsequently, acetic acid was added which induces the dissolution of calcium carbonate to liberate Ca^{2+}, CO_2, and H_2O by lowering pH (Fig. 5.1) (Lopes *et al.,* 2016; Poncelet *et al.,* 1995). Unlike external gelation technique, the gelation kinetics can be controlled by release and diffusion of Ca^{2+} ions (Lopes *et al.,* 2016). The released Ca^{2+} ions interacts with $-COO^-$ groups of alginate by partitioning internally to the formed aqueous alginate droplets. Hence, the gelation takes place within the formed droplets this process is termed as internal gelation (Poncelet *et al.,* 1995). The beneficial aspect of internal gelation technique includes its scale up potential and use of non-toxic solvents and reagents which favors its pharmaceuticals, biological and food applications (Yadav *et al.,* 2017).

Liquid paraffin was used as oil phase due to its non-toxic nature in internal and external applications. Additionally, pharmacopoeia approved surfactants such as Span 80 and Tween 80 was used to ensure stability of emulsion during formulation (Tsirigotis-Maniecka *et al.,* 2016). However, the introduction of acid, dissolves and uniformly disperses Ca^{2+} ions yielding more homogeneous microsphere structure. Liberation of CO_2 introduces porosity to the structure (Leong *et al.,* 2016). Complexation of alginate microspheres with chitosan circumvents the homogeneity and porosity of structure. Heterogeneity in the structure was further added by the presence of two types of interactions *i.e.* SA-Ca (ionic interaction) and SA-CS

(polyelectrolyte complexation). Moreover, there exists competition between Ca^{2+} ions and NH_3^+ ions of chitosan for reacting with $-COO^-$ groups of alginate (Dai *et al.,* 2008). Depending on the formulations conditions some authors have reported chitosan forms coating over alginate while others have reported it forms matrix system (Zhang *et al.,* 2011). Thus, the use of CS fortifies the properties of Ca-SA microspheres which are going to be proved in the next section.

5.2.1.2. Screening of variables

CS-Ca-SA microspheres were formulated based on selected independent formulation variables and optimized on the basis of desired dependent response variable using PBFD. PBFD are widely applied for screening studies to identify most important variables influencing process out of a large number of variables by limiting number of experiments to 12 runs (Table 5.5).

Pareto plots disclosed most significantly influencing formulation variables on the responses (Fig 5.4). Out of seven independent formulation variables, only CT had shown non-significant effects ($p > 0.05$) on all dependent response variable. The significantly influencing variables included SA, AS, SC on PS; SA, CaC, PR on EE, SA, AS on burst release (B), SA, CS on $T_{80\%}$. The pattern of influence is depicted by 2D contour and 3D response surface plots as explained in next section (Fig 5.5). Linear equations were established, expressing each response as a function of formulation variables. ANOVA results indicated variations in values of dependent response variables as a consequence of significant role of formulation variables on it.

The summary of regression parameters and associated *p-values*, F-values are given in Table 5.6. The mathematical model generated for each response was found statistically significant ($p < 0.05$) at 95% confidence interval. The R^2 values reaching 100% and closeness of adjusted R^2 to actual R^2 for all the responses indicated excellent correlations amongst equations and experimental data.

5.2.1.3. Dependent response variables

5.2.1.3.1. Particle size

$$PS = 71.8 + 62.06SA - 2.5CS + 4.90CaC + 4.71PR - 35.22SC + 0.517CT - 0.06944AS$$

PS of CS-Ca-SA microspheres were observed in the range of 74 to 461 µm. The above mentioned linear equation for PS include only significant terms ($p < 0.05$) indicating no interaction between variables. High R^2 value of 98.65% value indicates reasonable agreement between forecasted and experimental results. Significant formulation variables, SA with positive coefficient had the positive effect on PS, whereas AS and SC having negative coefficient had negative effect on PS. An increase in polymer content increases the viscosity of aqueous droplets of w/o emulsion and thereby, decreases the extent of shrinkage due to water loss during stirring and drying processes, resulting in an increased microspheres size (Noppakundilograt *et al.,* 2015).

Table 5.5: Plackett-Burman Factorial Design for fabrication of CS-Ca-SA microspheres and corresponding experimental results.

Run	SA	CS	CaC	SC	CT	AS	PR	PS (µ)	EEOZ (%)	EEDX (%)	BOZ (%)	BDX (%)	TOZ (%)	TDX (%)
1	(+)	(-)	(+)	(-)	(-)	(+)	(-)	283±16.98	82.65±1.44	85.19±2.74	17.12±0.51	16.89±0.51	68.25±1.87	70.55±1.91
2	(+)	(+)	(-)	(-)	(-)	(-)	(+)	377± 22.62	73.93±2.70	76.18±2.65	15.43±0.46	14.12±0.42	72.96±2.14	74.56±2.17
3	(-)	(-)	(-)	(+)	(+)	(-)	(+)	158± 9.48	60.23±3.01	64.67±2.81	27.18±0.81	26.52±0.79	52.36±1.48	53.10±1.53
4	(+)	(-)	(+)	(-)	(+)	(-)	(+)	461±27.66	81.19±1.89	86.64±2.56	14.83±0.44	13.81±0.41	67.76±1.99	69.56±2.02
5	(-)	(-)	(+)	(+)	(-)	(+)	(+)	74±4.44	68.46±2.37	70.33±3.31	30.41±0.91	29.52±0.88	57.31±1.63	59.45±1.69
6	(-)	(-)	(-)	(-)	(-)	(-)	(-)	195±11.7	65.39±2.88	68.12±3.11	25.65±0.76	24.38±0.73	54.81±1.55	56.75±1.61
7	(-)	(+)	(-)	(-)	(+)	(+)	(-)	108±6.48	64.82±2.98	66.29±2.98	28.78±0.86	27.63±0.82	56.01±1.55	57.23±1.62
8	(+)	(+)	(-)	(+)	(-)	(+)	(+)	252±15.12	67.37±1.31	69.84±3.23	20.29±0.61	19.92±0.59	72.50±2.09	73.28±2.13
9	(-)	(+)	(+)	(-)	(+)	(+)	(+)	134±8.04	66.17±2.43	68.21±2.91	35.13±1.05	34.14±1.02	62.64±1.82	64.88±1.85
10	(+)	(+)	(+)	(+)	(+)	(-)	(-)	349±20.94	84.73±2.16	87.67±2.91	12.71±0.38	11.71±0.35	76.28±2.15	77.28±2.22
11	(-)	(+)	(+)	(+)	(-)	(-)	(-)	172±10.32	67.92±2.45	69.91±2.93	27.19±0.81	26.32±0.78	59.07±1.66	60.67±1.73
12	(+)	(-)	(-)	(+)	(+)	(+)	(-)	236±14.16	77.75±2.22	79.47±1.85	22.03±0.66	21.44±0.64	66.80±1.97	68.76±2.12

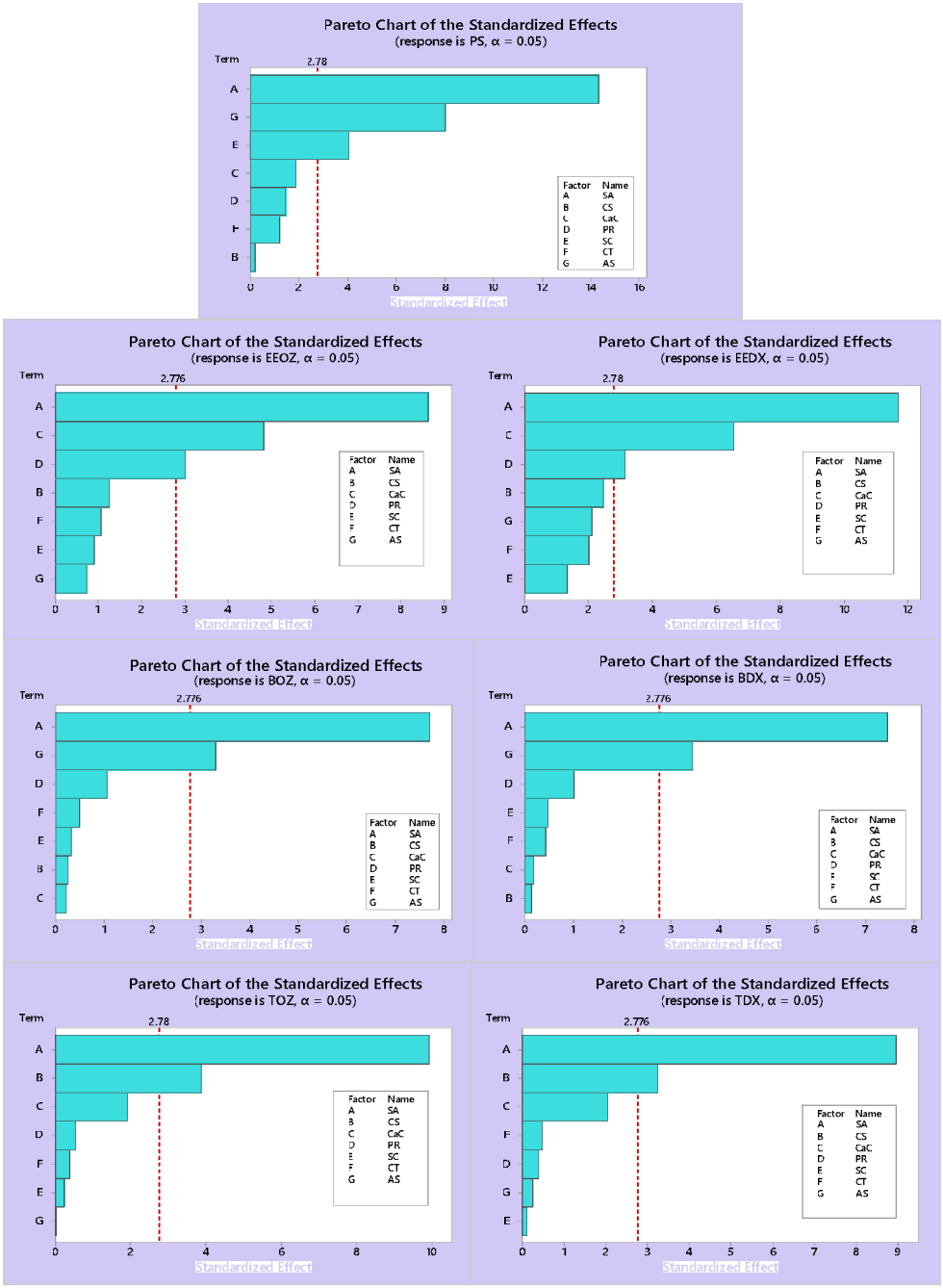

Figure 5.4: Demonstration of Pareto plots for the selection of critical formulation variables having significant effect on desired dependent response variables.

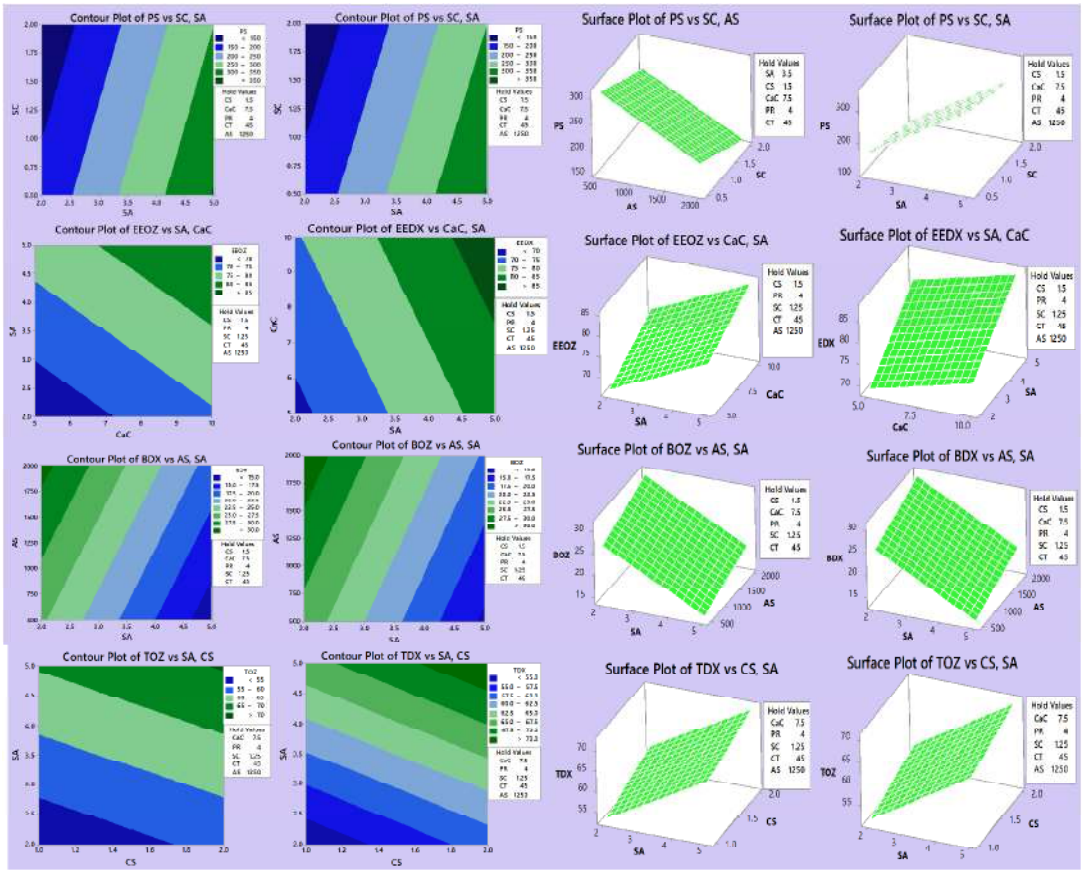

Figure 5.5: 2D Contour and 3D surface plots describing most influencing variables on particle size (PS), entrapment efficiency (EE), burst release (BOZ and BDX) and time for 80% cumulative drug release ($T_{80\%}$).

Conversely, high AS and high SC offered decrement in PS. Larger SC provides interfacial stabilization against coalescence of particles and thereby, results in smaller average microspheres. Moreover, high agitation speed imparts the force of breakdown to aqueous emulsion droplets leading to formation of small particles and *vice-versa*. These effects are well elaborated by contour and surface plots (Fig. 5.5). The parallel line of contour plots indicates linear relationship and lack of any interaction among variables.

Table 5.6: Summary of ANOVA results and regression parameters

Regression parameters	PS	EEOZ	EEDX	BOZ	BDX	TOZ	TDX
Actual R^2 (%)	98.65	96.51	98.09	94.73	94.52	96.71	95.98
Adjusted R^2 (%)	96.28	90.40	94.76	85.50	84.92	90.96	88.94
S value	22.57	2.49	1.91	2.69	2.73	2.39	2.63
Adjusted MS	21215	98.45	107.47	74.46	73.68	96.42	95.02
Adjusted SS	148505	689.20	752.29	521.24	515.78	674.98	665.15
Degrees of freedom	7	7	7	7	7	7	7
F value	41.65	15.79	29.39	10.27	9.85	16.80	13.64
p-value	0.001	0.009	0.003	0.02	0.022	0.009	0.012

5.2.1.3.2. Entrapment efficiency

Following linear equation represents the expression of EE as a function of independent variables.

EEDX = 55.81 + 4.303 SA - 2.72 CS + 1.446 CaC - 0.866 PR - 0.971 SC + 0.0743 CT - 0.001540 AS

EEOZ = 53.43 + 4.146 SA - 1.79 CS + 1.388 CaC - 1.080 PR - 0.854 SC + 0.0509 CT - 0.000686 AS

EEOZ and EEDX for prepared microspheres varied from 60.23 to 84.73% and 64.67 to 87.67% respectively. EE model was significant ($p < 0.05$) with high R^2 value of $> 90\%$. From linear equations, CaC and SA concentrations are directly proportional to EE due to positive values of coefficients while PR is inversely proportional to EE due to the negative value of coefficients. This effect is well correlated with surface and contour plots (Fig 5.5). Increased polymer (SA) has increased entrapment of drugs owing to increase in viscosity of dispersed phase droplets which restricts the leakage of the drug to the dispersion medium and *vice-versa* (Zeeb *et al.,* 2015).

Presumably, higher CaC has also increased EE by increasing the crosslinking networks and decreasing drug diffusion to the dispersion medium (Noppakundilograt *et al.,* 2015). Reduced EE was observed with increase in aqueous:organic PR due to drug leakage during aggregation of droplets and formation of less stable emulsion. Also, an increase in PR may had produced substantial reduction in viscous diffusional barrier (due to relative decrease in polymer concentration and viscosity), which would have favored the drug partition in external dispersion medium.

5.2.1.3.3. Drug release parameters

In polymer controlled drug delivery, drug release pattern can be characterized with burst effect and controlled effect as critical parameters for studying the onset of action and duration of action respectively. The linear equations obtained for burst release (BOZ and BDX) and $T_{80\%}$ are as follows;

$$BOZ = 29.52 - 3.996SA + 0.39CS - 0.066CaC + 0.408PR + 0.32SC + 0.0254CT + 0.00342AS$$

$$BDX = 28.22 - 3.923SA + 0.21CS - 0.054CaC + 0.402PR + 0.50SC + 0.0228CT + 0.00363AS$$

$$TOZ = 35.62 + 4.575\ SA + 5.36\ CS + 0.529\ CaC + 0.180\ PR + 0.210\ SC - 0.0169\ CT + 0.000030\ AS$$

$$TDX = 37.81 + 4.551\ SA + 4.95\ CS + 0.624\ CaC + 0.150\ PR - 0.11\ SC - 0.0247\ CT + 0.00025\ AS$$

Burst release *viz.* BOZ and BDX varied from 12.71 to 35.13 (%), 11.71 to 34.14 (%) respectively. TOZ and TDX ranged from 52.36 to 76.28 (h) and 53.10 to 77.28 (h) respectively for all formulated batches. Burst effect was significantly influenced by SA concentration and AS whereas $T_{80\%}$ was significantly affected by SA concentration and CS concentration as depicted in Pareto charts (Fig. 5.4).

From equations, it is clear that burst effect is inversely related to SA concentration and directly related to AS. This pattern is ascribed to an increase in entrapment of drugs on increasing SA as lesser drug was available for burst release. In a similar pattern, on increasing agitation smaller particles are formed and might

lead to lower entrapment of drugs which in turn increases the burst release. Alternatively, $T_{80\%}$ had direct relation with SA and CS concentrations. The increment in both polymer (SA and CS) concentrations had offered more matrix and crosslink network causing slow release of entrapped antimicrobials. This action in turn had produced prolonged and controlled release of drugs for approximately120 h.

5.2.1.4. Optimization of microspheres

Optimum formulation was selected based on the criteria of obtaining the minimum particle size and burst release, and maximum entrapment and $T_{80\%}$. The independent formulation variables obtained for optimized batch are as follows; SA - 5% (w/v), CS - 2% (w/v), CaC - 5% (w/v), PR - 1:2, SC - 1% (w/v), CT – 30 min, AS - 2000 rpm with composite desirability (D) of 0.7309 (Table 5.7). Experimental values then validated the predicted responses and corresponding% bias was calculated which was found within accepted limits (< 15%).

Table 5.7: Comparison of predicted and experimental values for validation of model

Responses	Predicted value	Experimental value (*mean±SD)	Bias (%)
PS (µm)	241.67	257±0.56*	5.966
EE (%)	81.12	79.89#	-1.538
B (%)	13.88	14.36#	3.342
$T_{80\%}$ (h)	74.10	72.43#	-2.305

Average value calculated for both drugs (OZ and DX).

5.2.1.5. Characterization of Optimized batch

5.2.1.5.1. Drug release and kinetics

In-vitro drug release study was performed in order to assess the potential of microspheres to control the release of drugs for prolonging its action. The *in-vitro* drug release profiles of OZ and DX from optimized microspheres in PBS pH 6.8 are shown in Figure 5.6.

The profile exhibits initial burst release and then extended release for up to 120 h. Burst release might likely be due to the rapid diffusion and desorption of surface adsorbed or weakly bounded drugs, immediately after microspheres comes in contact with dissolution medium. It acts as loading dose especially for treatment of antimicrobial infections. Further, it has been studied that CS-Ca-SA microspheres exhibited prolonged release, which is more probably due to stabilizing effect of phosphate ions on polycation salts (chitosan) (Liu *et al.,* 1997).

Aforementioned researchers have elaborated the role of three types of ionic interactions occurring in CS-Ca-SA microspheres which controls swelling, drug release and kinetics of drug release. They are; i) between oppositely charged $NH_3^+$of CS and $-COO^-$ groups of SA; ii) between Ca^{2+} and SA; iii) interchain hydrogen bonds. Therefore, the final structure and behavior of microspheres is governed by all these interactions.

The mechanism of drug release through the mathematical modelling of drug release data was evaluated. The kinetic parameters (R, K and n) were obtained after fitting the kinetic models to the *in-vitro* drug release data (Table 5.8). The drug release data of the microspheres were found in good correlation with Higuchi model ($R^2 = 0.98$) revealing matrix controlled drug release from microspheres. The results are in agreement with findings of Zhang *et al.,* (2011). This phenomenon could be ascribed to the mild solidification and low networks formed in the first-step which produced loose structure with high permeability. Chitosan moves inside the particles *via*. created pores and forms matrix system during second step of formulation. Further, release mechanism was determined from release exponent 'n' values using Korsmeyer-Peppas model. The values 'n' was more than 0.43, indicating non-Fickian type of drug release mechanism (Table 5.8).

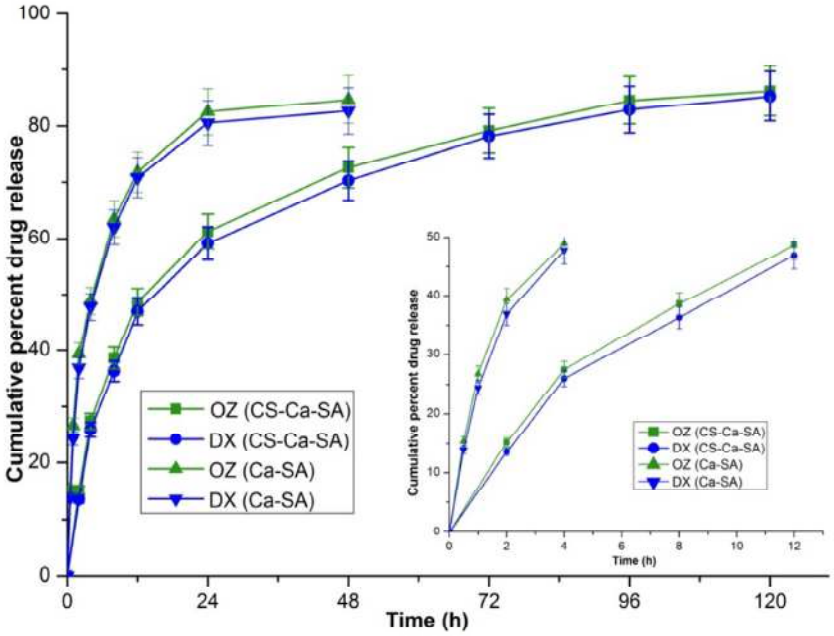

Fig 5.6: *In-vitro* release of OZ and DX from optimized CS-Ca-SA microspheres in PBS pH 6.8 using dialysis method. Inset showing the burst release profile within 12 h. Vertical bars indicate SD (n = 3).

Table 5.8: Drug release kinetics of OZ and DX from CS-Ca-SA and Ca-SA microspheres.

Microspheres		Zero-order Model		First-order Model		Higuchi Model		Hixson-Crowell model		Korsmeyer-Peppas model		
		R^2	K (mgh/ml)	R^2	K (h^{-1})	R^2	K ($h^{-1/2}$)	R^2	K ($h^{-1/3}$)	R^2	K (h^{-n})	n
CS-Ca-SA	OZ	0.901	1.97	0.755	0.02	0.976	13.25	0.944	0.04	0.971	1.34	0.56
	DX	0.893	1.92	0.739	0.02	0.971	12.91	0.934	0.04	0.963	0.51	0.58
Ca-SA	OZ	0.889	5.79	0.734	0.06	0.968	21.80	0.936	0.13	0.962	3.07	0.49
	DX	0.898	5.87	0.741	0.07	0.974	22.07	0.941	0.13	0.968	1.13	0.52

Diffusion Coefficient (cm^2/sec)			
CS-Ca-SA microspheres		Ca-SA microspheres	
OZ	DX	OZ	DX
8.66×10^{-4}	3.29×10^{-4}	15.73×10^{-4}	6.07×10^{-4}

In non-Fickian mechanism the drug release is controlled by diffusion of drugs as well as swelling of hydrophilic polymer chains of CS and SA (Ma *et al.,* 2008; Martinez *et al.,* 2013). A high value of diffusion coefficient (D) for OZ and DX indicates their greater tendency of diffusion contributed by hydrophilic polymers. The diffusion coefficient in the case of CS-Ca-SA microspheres was lower because of increased polymer concentration (CS+SA). Higher the value of diffusion coefficient corresponds to higher density of polymer matrix as compared to Ca-SA microspheres (Pasparakis and Bouropoulos, 2006).

5.2.1.5.2. Microscopic studies

SEM images of crystalline drug particles of OZ and DX are depicted in Fig. 5.7a and 5.7b respectively. Further, The SEM images of CS-Ca-SA microspheres shows particles were less spherical and more pear shaped (Fig. 5.7 c, d, e, f). Presence of little free drug particles and polymer deposits adds roughness to the surface the microspheres (Fig. 5.7). Studies conducted by Chan *et al.,* (2009), demonstrated the important role of concentration of polymers and distance of dropping alginate solution on the size and shape of microspheres (Chan, 2011). Nevertheless, these factors were kept constant. Surface depressions present on the surface were formed by solvent evaporation during drying process (Mladenovska *et al.,* 2007). EDXA plots helped in determination of elemental composition of microspheres (Fig. 5.8).

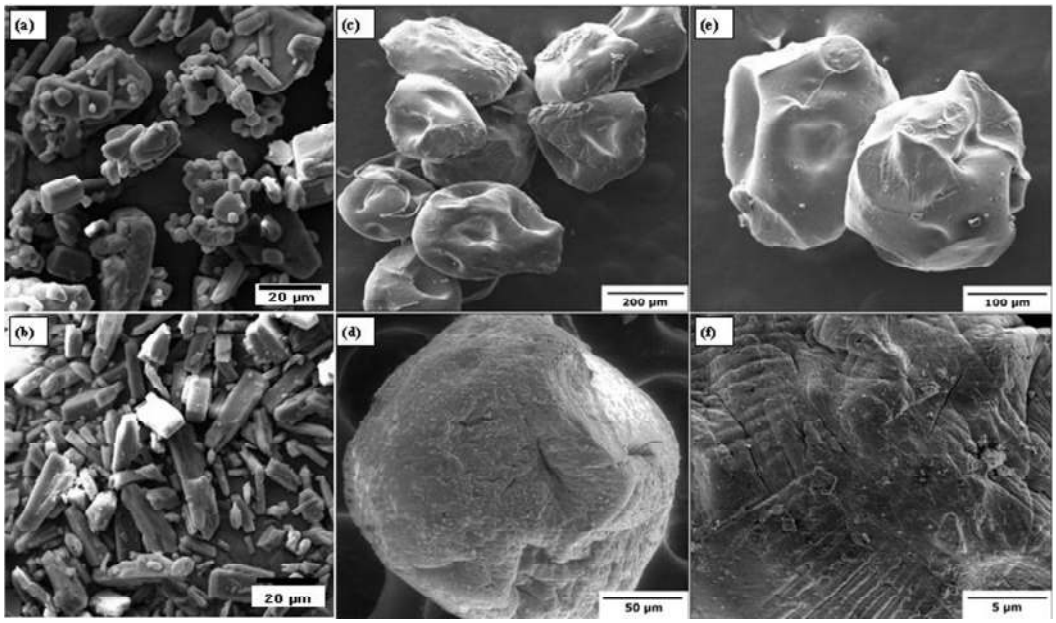

Figure 5.7: SEM images of (a) OZ powder; (b) DX powder; (c, d, e) CS-Ca-SA microspheres and (f) surface view of microsphere.

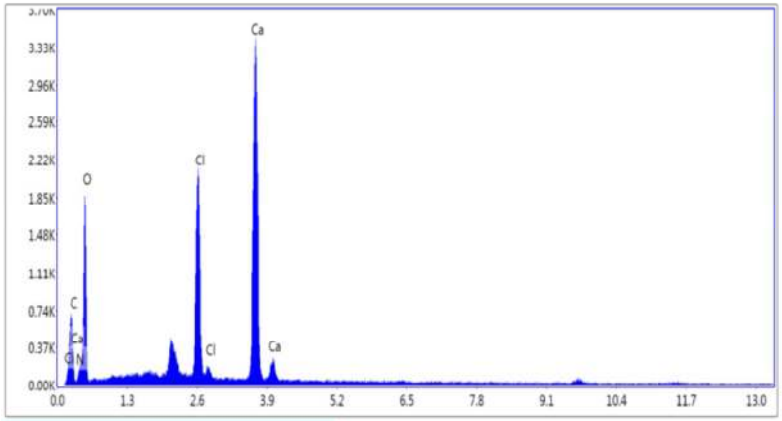

Element	Weight %	Atomic %
C	10.27	21.99
N	9.30	12.93
O	46.55	52.28
Cl	9.29	4.9
Ca	24.59	7.89

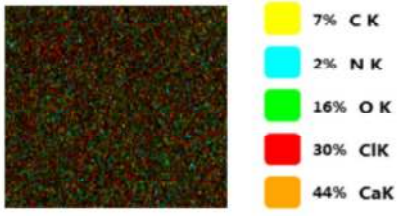

Fig 5.8: EDXA spectra showing elemental composition of CS-Ca-SA microspheres.

All elements belonging to both drugs and polymers were found uniformly dispersed in the matrix of microspheres. Also, presence of peaks of calcium ion indicated that calcium ions are also present in microspheres. This confirms the assumed composition as CS-Ca-SA microspheres.

5.2.1.5.3. FTIR

Infrared spectra of drugs and excipients were obtained as a plot between% transmittance and wavenumber (cm^{-1}) (Fig 5.9). The characteristic peaks of CS were achieved at 3424 cm^{-1}, 2876 cm^{-1}, 1655 cm^{-1}, 1599 cm^{-1} corresponding to the -NH_2, -OH stretching, carbonyl (C=O) stretching of the secondary amide (amide I band), and bending vibrations of the N-H (N-acetylated residues, amide II band) respectively.. The peaks observed at 1081 cm^{-1} and 1033 cm^{-1} were contributed by C-O stretching of secondary –OH and primary –OH groups of CS (Li *et al.,* 2008a).

In the infrared spectrum of SA, bands around 1030 cm^{-1} (C-O-C stretching) are attributed to its saccharide structure. Moreover, two strong absorption peaks at 1611 cm^{-1} and 1415 cm^{-1} belongs to asymmetrical and symmetrical stretching vibrations of the -COO- group, respectively. A little shifting of asymmetrical stretching peaks to 1637 cm^{-1} and symmetrical stretching peaks to 1415 cm^{-1} were observed in CS-Ca-SA microspheres. In addition, the absorption band of CS at 1599 cm^{-1} was shifted to 1559 cm^{-1} and 3424 cm^{-1} was shifted to 3448 cm^{-1} after the reaction with SA. These alterations and shifting in the peaks of CS and SA evidence the crosslinking of ammonium ions of CS to carboxylate ions of SA *via.* electrostatic interactions to form polyelectrolyte complexes (Ribeiro *et al.,* 2005).

The peculiar peaks of drugs as mentioned in *sub-section 4.2.1* (Chapter 4) are conserved in CS-Ca-SA microspheres but were absent in placebo CS-Ca-SA microspheres. Physical mixtures and optimized microspheres exhibited all the identifying peaks of OZ, DX and polymers disclosing the lack of any type of interaction between drugs and polymers before or after formulation.

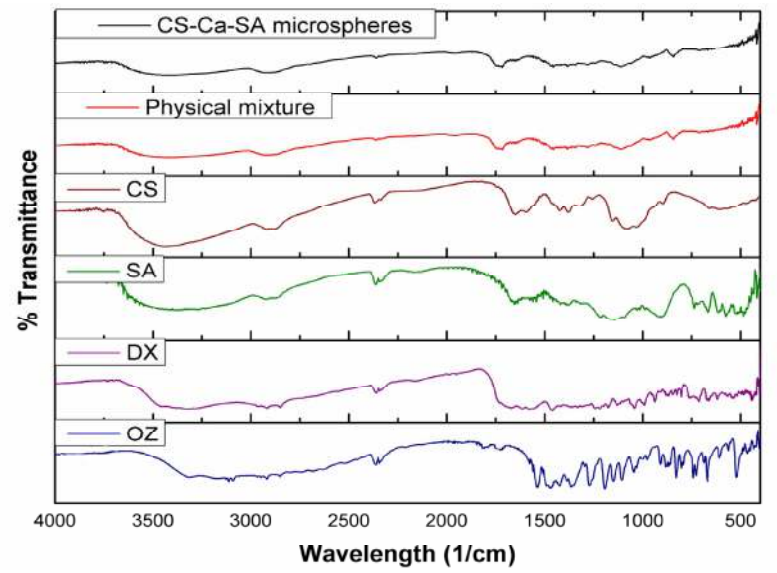

Figure 5.9: FTIR spectra of OZ, DX, CS, SA, physical mixture and CS-Ca-SA microspheres.

5.2.1.5.4. Differential Scanning Calorimetry

The DSC thermograms of drugs and polymers were recorded between intensity and temperature (Fig 5.10). SA and CS exhibited endothermic peaks at 86.6 °C and 72.0 °C respectively, contributed by dehydration of associated hydrophilic groups. In addition, the exothermic peaks at 250 °C for SA and 300 °C for CS resulted from degradation of polymers due to dehydration and depolymerization reactions. CS-Ca-SA microspheres exhibited broad endothermic and exothermic peaks formed due to coalescence of peaks of SA and CS. Previous studies explained the merging of CS and SA peaks occurred due to the interaction between them (Sarmento *et al.,* 2006). Exothermic peak observed at 250 °C is most probably due to degradation or partial decarboxylation of the protonated carboxylic groups and oxidation reactions of CS-Ca-SA microspheres.

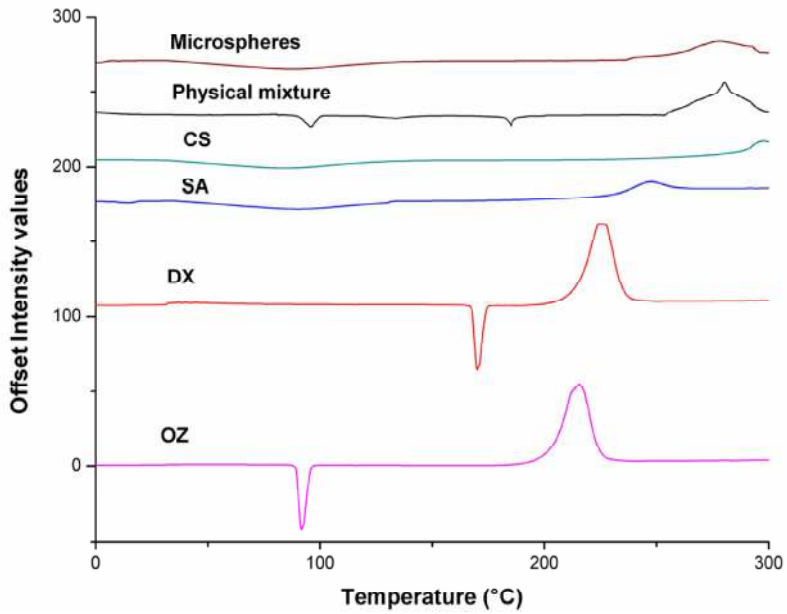

Figure 5.10: DSC graphs of OZ, DX, SA, CS, physical mixture and CS-Ca-SA microspheres.

OZ and DX thermograms recorded sharp melting endothermic peaks at 92 °C and 169 °C respectively corresponding to their crystal-lattice structure (5.7a, b, and Fig. 5.10). Microspheres showed flat curve and absence of any prominent endothermic peaks of drugs, which concludes that the drug has been transformed from crystalline state to amorphous state during the formulation. This also confirms the uniform dispersion of drugs into polymers without any interactions.

5.2.1.5.5. X-ray diffraction patterns

The sharp characteristic 2θ peaks in XRD spectra for OZ and DX explains their crystallite structure (Fig. 5.11). Characteristic 2θ peaks for OZ were observed at 11.88, 13.23, 14.86, 15.83, 18.39, 19.93, 20.77, 21.58, 22.11, 22.76, 22.97, 23.28, 23.91, 24.33, 24.60, 25.13, 25.37, 27.38, 28.66 and numerous minor peaks upto 45 (Desai and Dharwadkar, 2008). Similarly, characteristic 2θ peaks of DX are displayed at 10.381, 15.421, 17.461, 19.141, 19.701, 22.321, and 23.801 which helped in its identification. However, SA and CS do not present any diffraction peaks which confirm their amorphous nature and water-soluble properties. Besides,

microspheres formulated using drugs and polymers showed absence of any peak because of changes in crystallinity property of drugs. The lack of crystalline drugs peak in microspheres supports the results of DSC studies. The change in status of drugs from crystalline to amorphous forms is predominantly observed phenomenon ascribed to an increase in number of water molecules possessing higher degrees of freedom in the crystal structure (Mishra *et al.,* 2015). The outcomes of XRD and DSC studies complemented each other. Both indicated uniform dispersion of drugs into polymers and amorphous feature of microspheres.

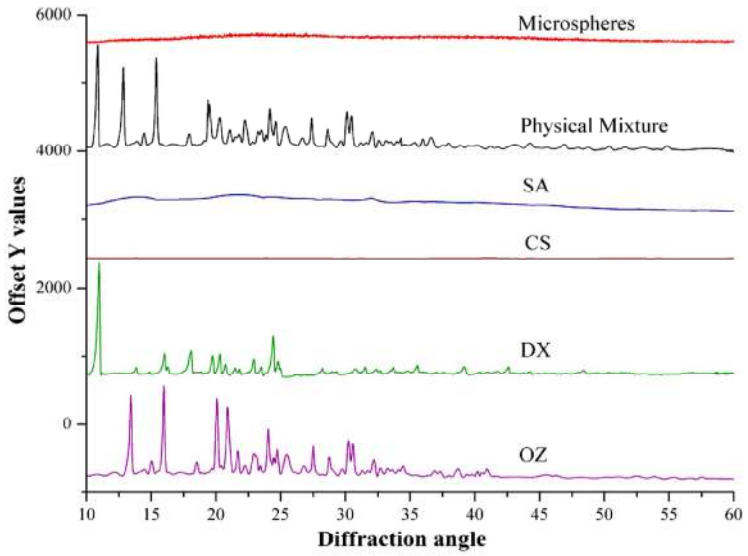

Figure 5.11: XRD pattern of OZ, DX, CS, SA, physical mixture and microspheres.

5.2.1.5.6. Swelling and erosion studies

Swelling is an important aspect related to polysaccharide polymers such as SA and CS. Swelling studies were done to determine the capability of increase in size of microspheres. Also, swelling behavior loosens the polymer networks and affects the drug release. The swelling behavior is dependent on relaxation of polymer networks due to differences in osmotic pressure inside the microspheres and outside buffer. The swelling was continued till equilibrium between osmotic pressure and forces of the crosslinking bonds were attained. When these two forces were equal,

water absorption within microspheres stops and maximum swelling is achieved (Pasparakis and Bouropoulos, 2006).

The swelling and erosion studies were conducted for whole drug release period of 120 h. It was observed that maximum swelling was attained within one day (Fig 5.12). After a certain point, decrease in swelling curve and erosion curve (due to rise in weight loss) was observed corresponding to dissolution and erosion of polymers. When compared to Ca-SA microspheres the CS-Ca-SA showed less swelling and more erosion at all-time points due to formation of additional crosslink networks that restricts the unwanted excess swelling. Excessive swelling of polymers initiated its breakdown of networks and erosion. Besides, at pH 6.8 alginates undergo ionization to liberate $-COO^-$ ions which repel electrostatically and cause relaxation of crosslink networks. This clearly results in increased water uptake which further facilitates swelling and breakdown of networks in Ca-SA microspheres.

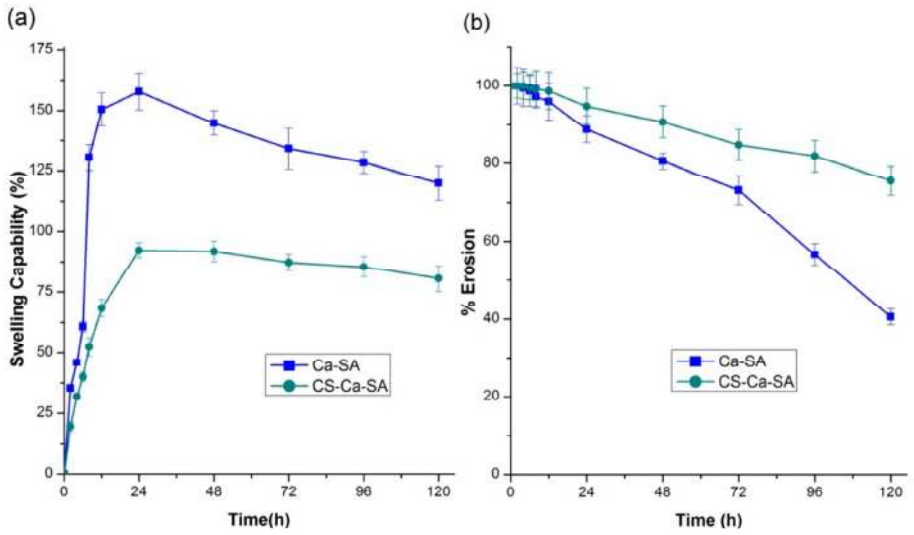

Fig 5.12: Comparative (a) swelling curve and (b) erosion curve of optimized batches of Ca-SA and CS-Ca-SA microspheres in simulated saliva pH 6.8. Vertical bars corresponds to SD (n = 3).

Additionally, the rapid swelling of Ca-SA resulted from competitions between phosphate ions present in simulated saliva or phosphate buffer and carboxylates of alginates of Ca-SA microspheres for calcium ions. The binding affinity of calcium for

phosphate ions to form calcium phosphate is more than that of carboxylate group. This chelating action of phosphate also leads to disruption and biodegradation of Ca-SA microspheres matrix in pH > 5 (Xu *et al.,* 2007). On contrary, chitosan exhibits lower degree of ionization and non-solubility at neutral pH, therefore, overcomes rapid swelling and erosion, which further increases the stability of microspheres.

5.2.1.5.7. Surface pH

pH of intrapocket formulations is an important factor to be studied. Extreme pH conditions causes damage and irritation to the oral mucosa. In particular, formulations with pH 6 to 7 are acceptable for oral mucosal and periodontal pocket administrations due to closeness of pH values to GCF and saliva (Marques *et al.,* 2011). The surface pH of optimized batch of CS-Ca-SA microspheres was 6.5±0.45 and Ca-SA was 6.6±0.67. In both cases it was near neutrality and closer to the pH of GCF and acceptable for internal use.

5.2.1.5.8. In-vitro mucoadhesion

Mucoadhesion is an important criterion for prolonged stay of microspheres at its site of action. Optimized batch (CS-Ca-SA microspheres) showed good mucoadhesivity with about 78.48±0.49% microsphere remained adhered to mucosal surface after washing. On the other hand, Ca-SA showed a lower mucoadhesion of 62±0.67% than CS-Ca-SA. This result supports the retention of microspheres for extended time into periodontal pockets regardless of GCF flow. Such high mucoadhesive property of microspheres was contributed by cationic nature of chitosan due to ammonium ions on the surface. As studied earlier, Ca-SA microspheres have negative charge on the surface because of presence of carboxyl group on the alginate surface. The addition of CS neutralizes the negative charges on the surface and develops positive charge attributed to excessive amino groups. These ammonium ions finds affinity to negatively charged mucus membranes (Zhang *et al.,* 2011). Thus, enhancement in retention of CS-Ca-SA microspheres was observed on the mucosal surfaces.

5.2.1.5.9. Antimicrobial activity

Zones of inhibitions created by antibiotics indicate their effectiveness against that particular microorganism. Drug release samples collected at different time points during release studies were evaluated for their antimicrobial potency against *S. aureus* and *E. coli* by determining zone of inhibition (Fig 5.13). A significant ($p < 0.05$) zone of inhibition had been observed indicating good activity of samples for both organisms. The sample collected at 12 h corresponds to burst release of drugs and could be well correlated with the significant zone of inhibition desirable for initiation of antimicrobial action. In all cases the concentrations of drug released was higher than that of desirable concentration required for inhibition of *S. aureus* and *E. coli* for drugs (Pei *et al.,* 2008; Wüst, 1977).

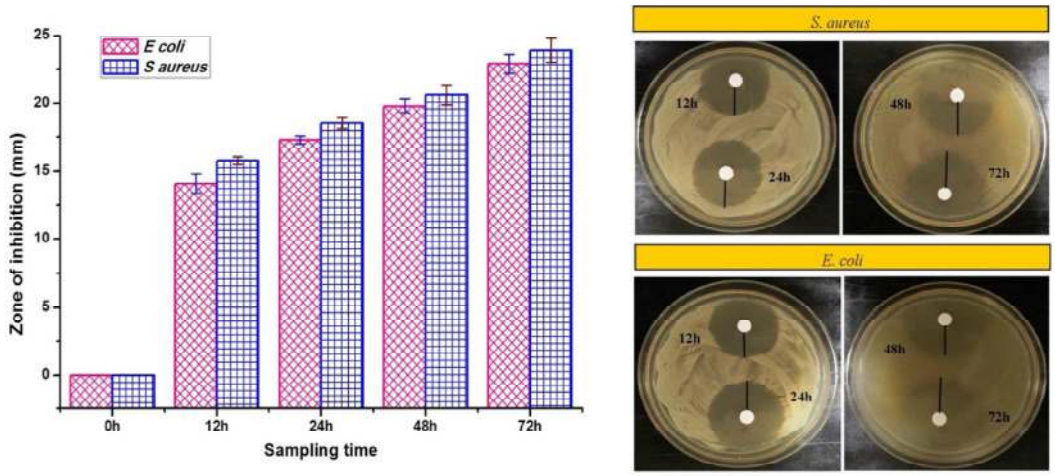

Figure 5.13: Antimicrobial activity of CS-Ca-SA microspheres against *S. aureus* and *E. coli*. Vertical bars represent SD, n=3 All groups showed significant ($p < 0.001$) zone of inhibition as compared to control (0h) by two-way ANOVA followed by Bonferroni post-tests.

Moreover, the zone of inhibitions of samples increased with time of sampling due to higher antibiotic concentration, indicating antimicrobial activity of drugs is dose dependent. Also, the outcomes of study revealed higher activity of samples for *S. aureus* than *E. coli*. Many previous studies have elaborated role of chitosan as antimicrobial agent. The investigations performed confirmed the effectiveness of fabricated microspheres in chronic infections such as periodontitis.

5.2.1.5.10. Cytocompatibility

Cytocompatibility testing is an important aspect for implantable biomaterials, and medical devices at an early stage. SRB is a negatively charged bright pink aminoxanthine dye taken by basic amino acids in the TCA fixed cells and colorimetric evaluation provides an estimate of total protein mass which is directly proportional to cell number. The greater the number of cells, the greater amount of dye is taken up and, after fixing, when the cells are lysed, the released dye will give a more intense color and greater absorbance (Houghton *et al.,* 2007).

The SRB assay was used to evaluate the effects of drugs on the metabolic activity of mice fibroblast cells L929. Microspheres samples showed cytocompatibility with L929 cell lines (Fig 5.14a) and high cell viability was observed in all samples (A, B and C). The samples showed non-significant difference ($p < 0.05$) in percent viability as compared to control indicating their safety for periodontal cavity application. Previous studies have indicated positive influence of SA and CS particles on cell proliferation (Borges et al. 2006).

Furthermore, to determine anti-proliferative effects of microspheres IC50 values were determined. Very high values of IC50 values were obtained at different incubation times of 24 h (3829.42 mg/ml), 48 h (3463.23 mg/ml), 72 h (2905.57 mg/ml), 96 h (2611.344 mg/ml) and 120 h (2197.57 mg/ml) (Fig 5.14b). These results ensure the long-term safety of microspheres for *in-vivo* applications. Though, IC_{50} values decreased with increasing incubation time. Apparently, various samples of microspheres (A, B and C) showed the substantial number of L929 cells when observed under fluorescent microscope as compared to control after incubation period of 120 h (Fig 5.14c).

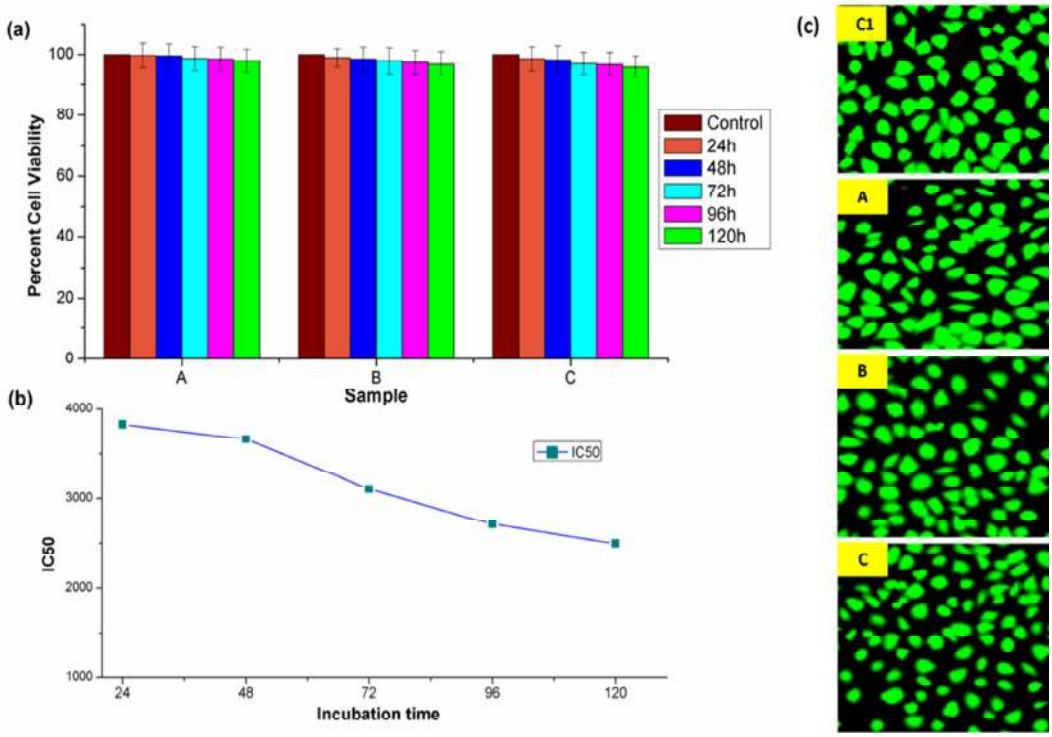

Figure 5.14: (a) Percent cell viabilities of microspheres samples, A (0.01 g/ml), B (0.05 g/ml) and C (0.1 g/ml) prepared by incubating in DMEM media for 120 h against L929 cell lines. Untreated DMEM media was evaluated as control. Vertical bars represent SEM (n = 6). All groups are compared with control two-way ANOVA followed by Bonferroni post-tests.; (b) Incubation time *vs.* IC_{50} plot; (c) fluorescent microscopic images showing cytocompatibility of various microspheres samples (A, B, C and control (C1)) with L929 cell lines stained with FDA and EDB.

5.2.1.5.11. Stability studies

Stability studies of optimized batch were performed at three different storage conditions (refrigeration, room temperature, and high temperature) to assess the potential of microspheres to withstand variable environmental conditions encountered during its transportation and storage. PS, EE and total drug content (TDC) were determined at predefined time intervals and compared with fresh samples during storage period (Table 5.9). PS and EE did not show any significant difference ($p > 0.05$) with variations in storage conditions.

The shelf-life of any drug or product is defined as the time at which the average drug characteristic *i.e.* potency remains within an approved specification after manufacture. The US Food and Drug Administration (USFDA) require that a shelf-life be indicated on the immediate container label of every drug product. Assay methods generally estimate the true shelf-life of products(Shao and Chow, 2001). Therefore, assay for drug content was performed and shelf-life was predicted as time in which TDC reaches 90% (LS) (Fig. 5.15).

For shelf-life of microspheres was found to be 19.87, 12.35 and 9.40 months when stored at refrigeration, room temperature and high temperature storage respectively (Fig 5.15). These outcomes are supported by Noppakundilograt *et al.,* (2015) that had shown longer product shelf-life and higher stability of eucalyptus oil after encapsulating into sodium alginate polymer (Noppakundilograt *et al.,* 2015).

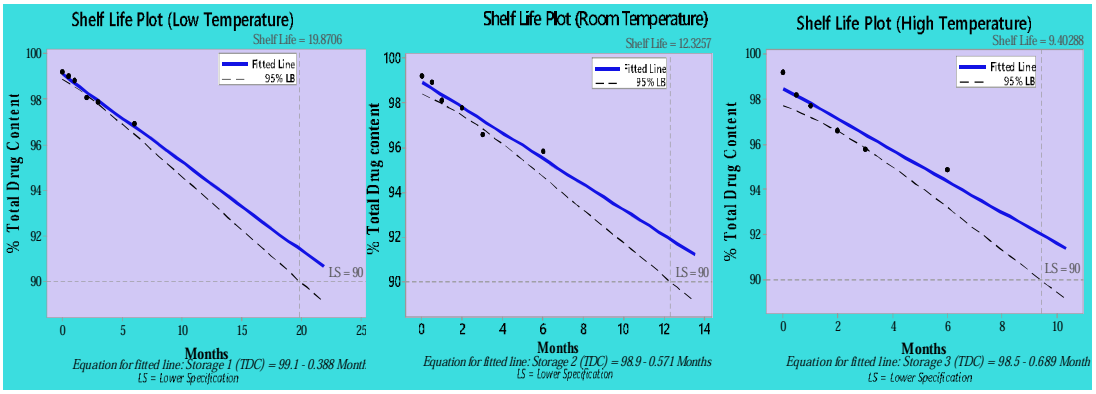

Figure 5.15: Shelf-life plots of optimized batch of microspheres at different storage conditions *viz.* Refrigeration, Room temperature, High temperature. LS - lower specification (set at 90%).

Table 5.9: Stability parameters obtained after six months of storage at different storage conditions.

Stability Parameters	Fresh Sample	Refrigeration	Room Temperature	High Temperature
Particle size	257±0.56*	256±0.28*	255.98±0.72*	252.45±1.12*
EE (%)	79.89#	78.45#	77.74#	75.29#
B (%)	14.36#	20.04#	20.87#	22.64#
$T_{80\%}$ (%)	72.43#	72.66#	71.19#	70.38#
TDC (%)	100	96.91±0.67*	95.84±0.43*	94.88±0.26*

#the values are average values obtained for both drugs.*mean±SD (n = 3).

5.2.2. Part B

5.2.2.1. Formulation of CSTPP microspheres

CSTPP microspheres were successfully formulated using ionic-gelation crosslinking method. Two methods employed were; direct ionic-gelation of CS with TPP to form microspheres (Method A) and indirect ionic-gelation (method B) where first w/o emulsion was formed and then was crosslinked into microspheres by addition of TPP (Figure 5.2 and 5.16). Chemically, ionic-gelation involves cationic-anionic type of interaction.

In *method A*, spontaneous crosslinking of CS solution containing drugs occured after addition of TPP causing precipitation of droplets into microspheres (Fig 5.2 and 5.16a). This method offers lower cost, uses economic excipients (no oil and surfactants used) and also is less time consuming. However, the formed gel particles were very weak and strengthened by continuous stirring for specified time so as to achieve complete crosslinked microspheres (Fig 5.16 b, c, d). In *method B*, solution of drugs and CS were prepared and mixed by homogenization. This aqueous mixture when added to oil phase containing surfactants forms w/o emulsion (Fig 5.16e). The aqueous droplets of emulsion were gelled by addition of TPP (Fig 5.16f). The gelled droplets were crosslinked by agitation to form microspheres (Fig 5.16 g,h).

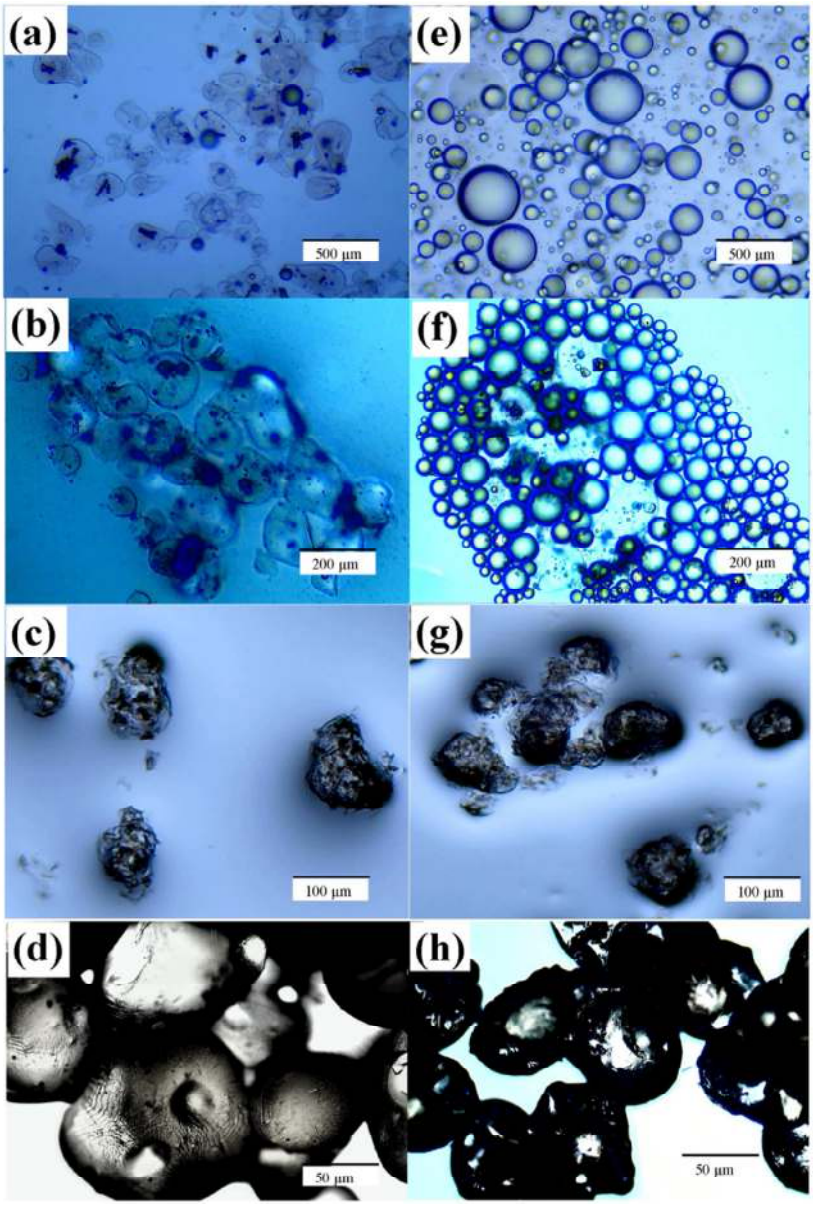

Figure 5.16: Optical microscopic images demonstrating process of formulation of microspheres. Method A - a) Immediate gelation of CSTPP particles, which appear weak and in variable sizes; b) Solidification of particles; c) Solidified microspheres; d) Dried microspheres: Method B - e) Formed w/o emulsion; f) solidification of aqueous chitosan droplets after addition of TPP, the solidified particles surrounded by surfactants bubbles; g) Solidified microspheres; h) Dried microspheres.

Nevertheless, the different pKa values of CS (6.8-7.2) and TPP (0.9, 1.9, 5.3, and 7.7), and opposite charges at different pH conditions governs the degree of

ionization and strength of interactions (Pati *et al.,* 2011). Prepared TPP and CS solution had pH of 8.4±0.21 and 2.8±0.23 respectively. At these pH conditions TPP exists as OH, HP_3O_4, and P_3O_5 while CS exists as H^+, CS-NH_4^+ ions.

Previous studies mentioned that complete ionic crosslinking takes place at lower pH condition where protonated amine groups of CS interact instantaneously with anionic groups of TPP through electrostatic attraction to form CSTPP crosslinks (Ko *et al.,* 2002; Koukaras *et al.,* 2012; Mi *et al.,* 1999; Pati *et al.,* 2011; Shu and Zhu, 2000). Therefore, for attaining complete crosslinking addition of TPP solution to CS solution has been preferred approach by researchers over reverse addition (Mi *et al.,* 1999; Shu and Zhu, 2000).

5.2.2.2. Experimental design and screening of variables

A total of 12 batches were formulated using seven variables at two levels (Table 5.10). The variations in results obtained for selected responses indicates significant role of independent variables on responses. The summary of ANOVA results, associated *p-value* and regression parameters are given in Table 5.11. The mathematical models determined for each response was found statistically significant ($p < 0.05$) in each case and closeness of R^2 values to 100% for all the responses indicates excellent fit of equations to experimental data (Table 5.11). In addition, Pareto charts screened out the processing variables having significant influence on responses (Fig 5.17). The response surface or contour plots were employed to determine the correlations and interactions between chosen variables (Fig 5.18 and 5.19).

Table 5.10: A 12 run Plackett-Burman factorial design for fabrication of tripolyphosphate crosslinked chitosan microspheres. *Values are mean±SD, n = 3

RUN	MOP	CS	TPP	CT	AS	DT	PY* (%)	PS* (µm)	EEOZ* (%)	EEDX* (%)	BOZ* (%)	BDX* (%)	TOZ* (h)	TDX* (h)
1	(-)	(-)	(+)	(+)	(+)	(+)	77.65±4.61	75± 3.75	57.44± 2.87	65.23± 3.36	32.45±1.62	27.45± 1.37	30.57±1.52	41.61±2.08
2	(+)	(+)	(-)	(+)	(-)	(+)	92.34±4.31	221±11.05	86.63± 4.20	95.11± 4.75	19.43±0.97	17.43± 0.87	37.3±1.865	56.56±2.82
3	(+)	(-)	(+)	(+)	(-)	(-)	87.31±3.96	180± 9.10	72.51± 3.61	81.99± 4.14	25.55±1.27	22.54± 1.12	40.34±2.01	60.1±3.01
4	(-)	(+)	(+)	(+)	(-)	(-)	79.22±4.41	282±14.10	73.28± 3.56	81.63± 4.08	16.28±0.81	14.28± 0.71	52.25±2.61	70.24±3.51
5	(+)	(-)	(+)	(-)	(-)	(+)	89.29±4.52	222±11.10	74.81± 3.74	82.78± 4.23	29.87±1.49	27.87± 1.34	33.51±1.67	54.53±2.72
6	(+)	(+)	(+)	(-)	(+)	(-)	90.45±4.12	211±10.55	85.32± 4.34	94.14± 4.71	18.53±0.92	16.53± 0.83	45.17±2.25	64.15±3.20
7	(-)	(-)	(-)	(+)	(+)	(-)	82.41±5.04	102±5.15	55.56± 4.21	63.58± 3.28	35.39±1.82	34.39± 1.71	23.89±1.19	27.53±1.37
8	(+)	(+)	(-)	(+)	(+)	(+)	95.1± 4.75	176± 8.82	79.91± 2.77	87.27± 4.51	22.31±1.12	20.31± 1.02	43.12±2.15	60.1±3.01
9	(-)	(+)	(-)	(-)	(-)	(-)	84.17±4.20	315±15.75	66.1± 4.04	74.94± 3.85	25.61±1.28	23.61±1.18	39.83±1.99	55.8±2.79
10	(-)	(+)	(+)	(-)	(+)	(+)	80.57±4.02	272±13.61	72.86± 3.31	80.42± 4.02	17.54±0.78	15.54± 0.68	45.42±2.27	64.4±3.22
11	(-)	(-)	(-)	(-)	(-)	(+)	72.38±3.11	124±6.20	53.77± 3.54	62.67± 3.13	45.16±2.26	42.06± 2.11	16.53±0.82	26.42±1.32
12	(+)	(-)	(-)	(-)	(+)	(-)	86.59±4.07	82± 4.10	61.69± 3.58	70.46± 3.57	43.26±2.16	40.26± 2.01	21.61±1.08	24.14±1.20

Table 5.11: Summary of ANOVA of Plackett-Burman factorial design batches.

Responses	Regression Parameters				
	Actual R^2 (%)	**S value**	***p-value***	**Adjusted R^2 (%)**	**Predicted R^2 (%)**
PY	88.10	3.397	0.032*	73.83	61.48
PS	89.66	38.173	0.023*	77.26	70.47
EEOZ	97.22	2.764	0.001*	93.87	83.96
EEDX	97.26	2.739	0.001*	93.96	84.20
BOZ	95.47	3.095	0.003*	90.03	73.91
BDX	96.67	2.6003	0.002*	92.67	80.80
TOZ	95.17	3.530	0.004*	89.37	72.18
TDX	95.02	5.391	0.004*	89.04	71.29

*Statistically significant ($p < 0.05$).

5.2.2.2.1. Process yield

$$PY = 78.49 + 5.390MOP + 1.748CS - 0.354TPP + 0.0196CT + 0.00134AS + 0.0235DT$$

For all batches the PY was obtained in the range of 72 to 95% w/w indicating effects of processing conditions (Table 5.10). The Pareto charts reveals that MOP had maximum standardized effect while others variables did not have any significant effect on process yield (Fig 5.17). Further, method B gave higher yield than method A (as (+) level), attributed to use of w/o emulsification method where less loss of aqueous soluble drugs occurs due to use of non-aqueous solvent (paraffin oil).

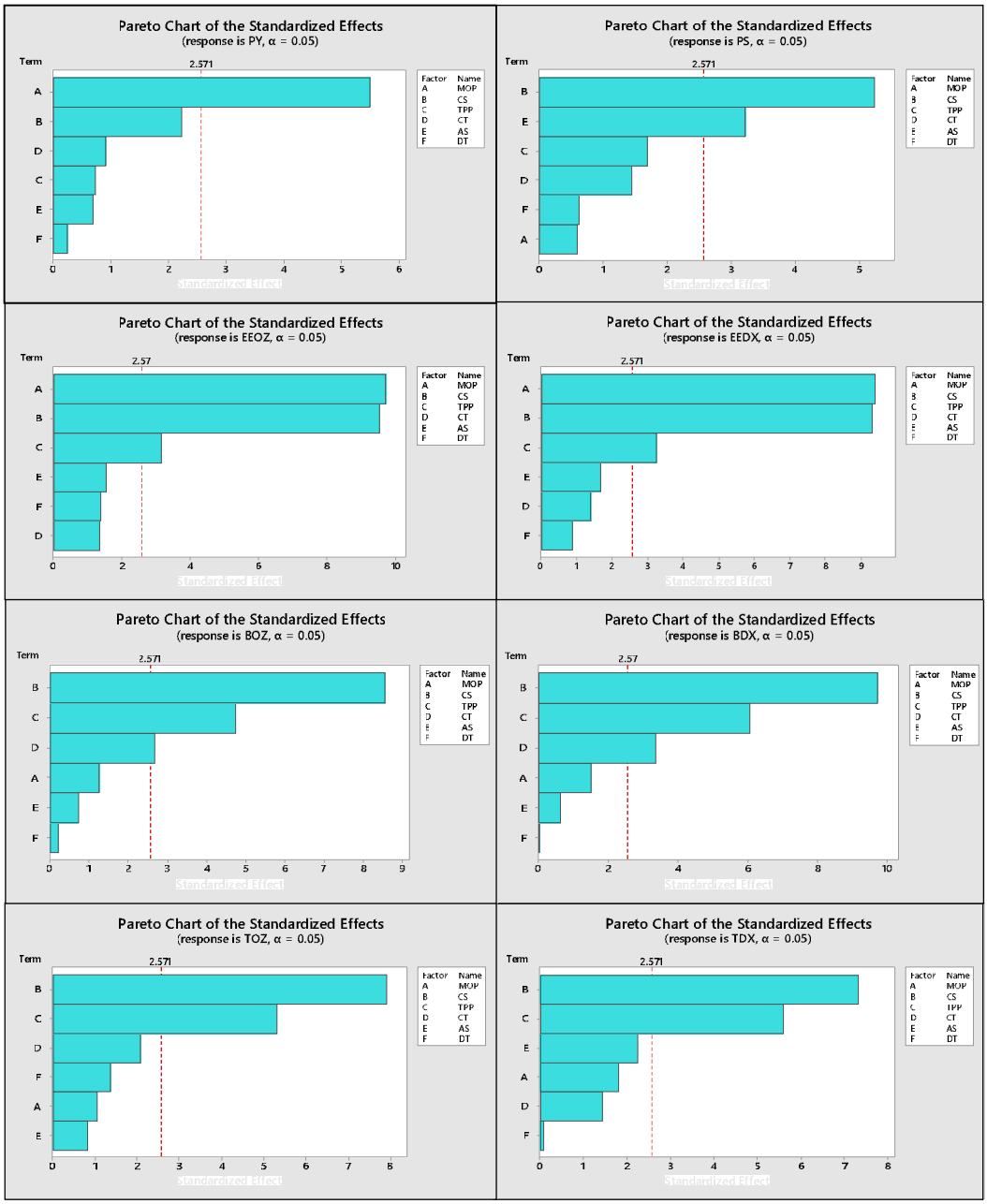

Figure 5.17: Pareto charts for process yield (PY), particle size (PS), entrapment efficiency (EEOZ and EEDX), burst release (BOZ and BDX) and time for 80% drug release (TOZ and TDX) indicating most influencing variables.

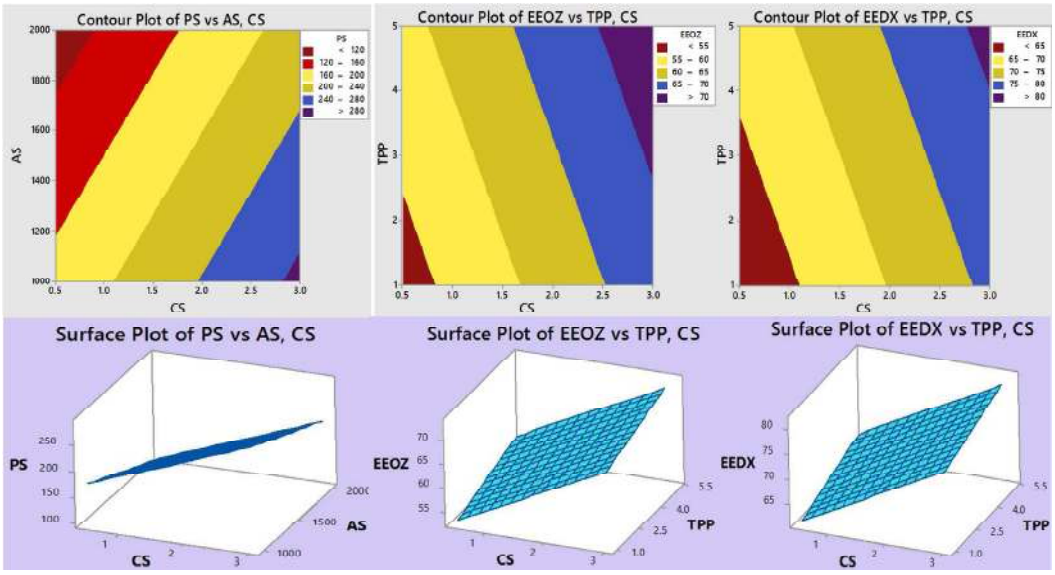

Figure 5.18: Contour and surface plots depicting the effect of independent variables on responses: particle size (PS) and entrapment efficiency (EEOZ and EEDX).

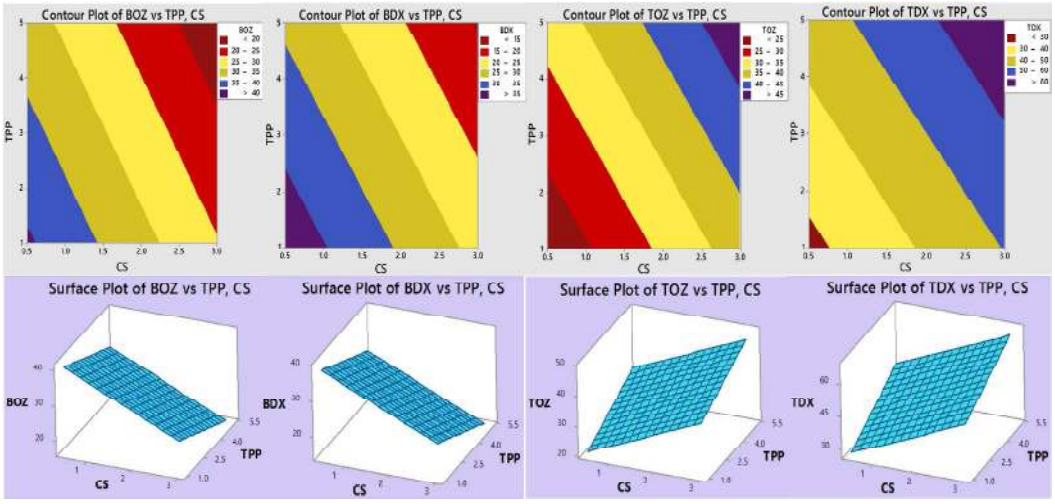

Figure 5.19: Contour and surface plots displaying the effect of independent variables on responses: burst release (BOZ and BDX) and time for 80% drug release (TOZ and TDX).

5.2.2.2.2. Particle size

The PS of microspheres ranged between 75 and 315 µm (Table 5.10). The relation between PS and various process variables is presented by following equation;

PS = 189.0 - 6.5MOP + 46.13CS + 9.25TPP - 0.352CT - 0.0710AS + 0.68DT

Analysis of data from Pareto charts and ANOVA, demonstrated that only the concentration of CS and AS had significant ($p < 0.05$) effects on PS (Fig 5.17, Table 5.10). The positive effects of CS can be explained as the concentration of CS increases the viscosity of CS solution increases resulting into formation of large droplets which gets hardened to form larger microspheres. Reportedly, the formation of CSTPP microspheres or nanoparticles is critically controlled by CS and TPP concentration ratios (Huang and Lapitsky, 2011; Koukaras *et al.,* 2012; Papadimitriou *et al.,* 2008). Since, intentionally higher concentrations of CS and TPP were used as compared to studies of Papadimitriou *et al.,* 2008 microspheres were produced irrespective of ratios of CS/TPP (Papadimitriou *et al.,* 2008).

5.2.2.2.3. Entrapment efficiency

EEOZ and EEDX values varied between 53 to 86% and 62 to 95% respectively irrespective of method of preparation (Table 5.10). Following regression equation represents the relations between EE of OZ and DX of microspheres with all independent variables (Table 5.10).

EEOZ = 60.90 + 6.822MOP +5.888CS + 1.357TPP + 0.0200CT - 0.00239AS - 0.0913DT

EEDX = 69.37 + 6.940MOP + 5.787CS + 1.340TPP + 0.0174CT - 0.00300AS - 0.0562DT

Pareto charts and ANOVA analysis showed significant ($p < 0.05$) dependence of EEOZ and EEDX on MOP, CS and TPP concentration (Fig. 5.17). Generated equations exhibited significant ($p < 0.05$) linear relationships of EE with CS and TPP. High CS concentration had contributed for enhancement in EE of both drugs by providing more matrix for drug entrapment. Likewise, higher TPP concentration had also increased the drug entrapment by creating more crosslink networks. Comparatively, higher entrapment was obtained for DX than OZ due to difference in their aqueous solubility. OZ is highly water soluble and loss of drug could have occurred during hardening and washing procedure. The effects of independent

variables (CS and TPP) on EE are well presented in 2D and 3D plots (Fig 5.18 and 5.19).

5.2.2.2.4. Drug release parameters

The *in-vitro* release profiles were further studied in terms of two critical parameters: Burst release (BBOZ and BBDX) and $T_{80\%}$ (TOZ and TDX).

Linear equations describing drug release parameters are as follows:

$$BOZ = 47.41 - 1.123MOP - 6.132CS - 2.122TPP - 0.0529CT + 0.00126AS - 0.0178DT$$

$$BDX = 45.12 - 1.123MOP - 5.839CS - 2.272TPP - 0.0559CT + 0.00093AS - 0.0012DT$$

$$TOZ = 10.51+1.05MOP + 6.443CS + 2.708TPP + 0.0470CT - 0.00166AS + 0.139DT$$

$$TDX = 28.64 + 2.80MOP + 9.13CS + 4.353TPP + 0.0494CT - 0.00695AS - 0.014DT$$

Concentration of CS and TPP possessed significant ($p < 0.05$) effect on burst and controlled release behavior of both drugs as depicted in Pareto charts and ANOVA (Fig. 5.17 and Table 5.11). Also, CT exhibited significant effect on burst release. The equations reveal CS and TPP are inversely related to burst release while directly proportional to $T_{80\%}$. Hence, burst release gets minimized on maximizing CS and TPP by bringing increased entrapment of both drugs as discussed in previous section. However, a little burst release is desirable in antimicrobial therapy for early achievement of MIC. Alternatively, high burst release will deliver high dose of drugs at once, which will affect controlled and slow release of drugs from microspheres.

Further, maximizing CS and TPP concentrations also accounts for increasing $T_{80\%}$ and provided more slow and prolonged drug delivery owing to increase in density of polymer matrix which decreases the diffusion of drug as reported by Remunan-Lopez and Bodmeier (1997) (Remunan-Lopez and Bodmeier, 1997). Higher concentration of CS increases the viscosity of solution while higher TPP increases crosslinking networks and further, diffusion of drug is slowed down. Increased viscosity of chitosan solution forms relatively strong walls of microspheres

upon interaction with TPP. Some authors had reported lower viscosity of CS forms weaker microspheres (Ko *et al.,* 2002; Lim *et al.,* 1997).

5.2.2.2.5. Optimization of CSTPP microspheres

Optimization of CSTPP microspheres were performed to find out optimum batch based on the criteria of attaining the minimum PS and burst release while maximizing PY, EE and $T_{80\%}$ using response optimizer tool (Table 5.12).

Table 5.12: Predicted and experimental values of responses for optimized batch of microspheres.

Variables	Optimized batch		Desirability
MOP	METHOD B		0.8747
CS	2.5%		
TPP	5%		
CT	120 min		
AS	2000 rpm		
DT	Freeze drying		
Responses	**Predicted value**	**Experimental value (mean±SD) (n = 3)**	**Bias* (%)**
PY (% w/w)	92.10	95.67±1.68	3.7315
PS (µm)	176.93	168.45±2.95	-5.0341
EEOZ (%)	84.55	85.56±1.25	1.1804
EEDX (%)	92.15	91.34±1.08	-0.8867
BOZ (%)	16.07	15.26±0.09	-5.3079
BDX (%)	13.16	12.91±0.28	-1.9364
TOZ (h)	46.98	47.09±0.67	0.2335
TDX (h)	67.70	67.95±0.33	0.3679

The independent variables obtained for optimized batch was as follows; method B, CS (2.5%), TPP (5%), CT (120 min), AS (2000 rpm), DT (freeze-dried) with composite desirability (D) of 0.8747. The software predicted responses were then validated by experimental values and % bias was calculated which was found within accepted limits.

5.2.2.3. Characterization of optimized CSTPP microspheres

5.2.2.3.1. Drug release kinetics

Figure 5.20 shows biphasic drug release manner of optimized batch with prolonged release for 120 days. Such biphasic release pattern with burst and controlled release is most commonly observed with microspheres (Pandey *et al.,* 2015). Burst release of drugs was observed due to presence of surface adsorbed drugs and controlled release was observed due to drugs entrapped within the matrix. Both drugs showed almost similar pattern of drug release as a result of their high water solubility.

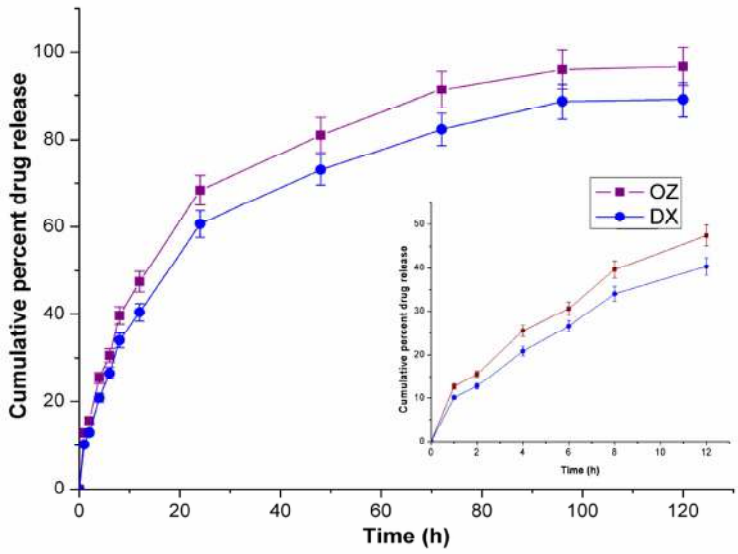

Figure 5.20: *In-vitro* drugs release profiles of optimized microspheres in phosphate buffer pH 6.8. Inset showing burst release pattern (Vertical bars represent mean value±SD, n = 3).

In-vitro kinetic analysis disclosed that drug release was best explained by Korsmeyer-Peppas equation with the highest value of linearity ($R^2 > 0.9$) than other models (Table 5.13).

Table 5.13: Release kinetics of drugs from optimized CSTPP microspheres.

Drugs	Zero-order Model		First-order Model		Higuchi Model		Hixson-Crowell model		Korsemeyer-Peppas model		
	R^2	K (mgh/ml)	R^2	K (h^{-1})	R^2	K ($h^{-1/2}$)	R^2	K ($h^{-1/3}$)	R^2	K (h^{-n})	n
OZ	0.867	1.445	0.686	0.015	0.972	0.079	0.937	0.037	0.99	0.117	0.555
DX	1.216	0.905	0.734	0.014	0.980	0.089	0.933	0.032	0.986	0.098	0.550
Diffusion coefficient (cm2/sec)											
OZ			7.78×10^{-4}				**DX**		6.24×10^{-4}		

The value of 'n' determined from Korsmeyer-Peppas equation was around 0.55 ($n > 0.43$) for both drugs which indicates the drug release followed non-Fickian (relaxation as well as diffusion controlled) mechanism. This points towards diffusion as well as swelling controlled drug release mechanism from hydrophilic CS. These results are supported by high values of diffusion coefficients for OZ (7.78×10^{-4}) and DX (6.24×10^{-4}) from CSTPP microspheres. Moreover, the drug release mechanism was independent of type of drugs and totally dependent on polymer and matrix of microspheres.

5.2.2.3.2. Swelling and erosion studies

The swelling and permeability characteristics of CS are function of release media pH and TPP concentration. Swelling of CS in water brings loosening of internal structure of microspheres promoting higher drug release. However, presence of TPP lowers the swelling capability of microspheres hence, lowers drug release (Fig 5.21). Maximum swelling of microspheres was achieved in 48 h after that no further significant swelling was observed. However, weight loss increased with time and about 25% erosion occurred in 120 h. This result also supports erosion controlled drug release mechanism as observed generally with hydrophilic polymers like chitosan.

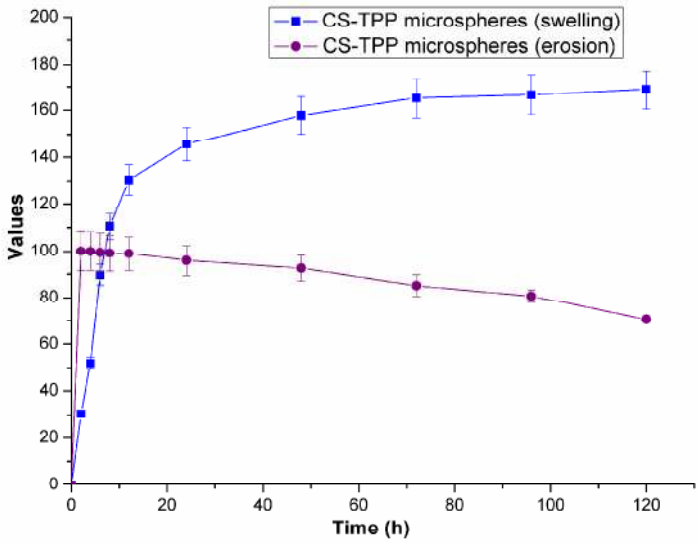

Fig. 5.21: Swelling (% swelling *vs.* time curve) and erosion (% drug remaining *vs.* time) curve for microspheres. Vertical bars represent SD.

5.2.2.3.3. Solid state characterization

5.2.2.3.3.1. Microscopic studies

The surface morphologies of CSTPP microspheres depicted rough surface and varied from oblong to spherical in shape depending on MOP and drying technique (Fig. 5.22). Optical microscopy studies showed the particles prepared by method A were rough, less spherical and aggregated. On the contrary, method B yielded porous, smooth and spherical microspheres.

In particular, it has been observed that drying conditions do not have any significant effect ($p > 0.05$) on the selected responses statistically. Nonetheless, microscopic studies observed that oven-dried particles were irregular and rough while freeze-dried particles were more spherical, porous and free-flowing with low degree of aggregation (Fig. 5.22d). Free flowing property of microspheres is desirable for accurate dosing (Lim *et al.,* 1997). Pores have been observed as created by evaporation of water during drying process. Past findings have indicated paramount role of surface porosity and roughness for mucoadhesive property of microspheres

(Govender *et al.,* 2005). FD is considered as most suitable method of drying, by inducing less structural damages particularly for thermolabile substances (Chan *et al.,* 2002).

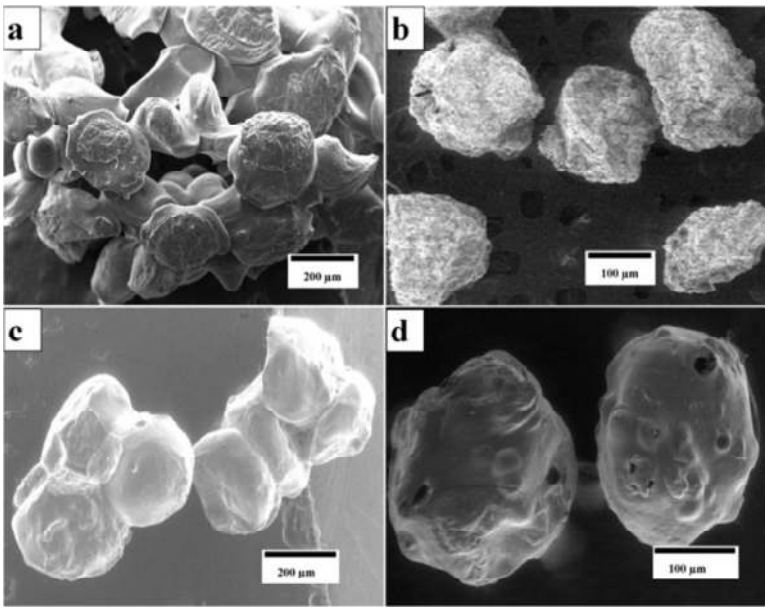

Figure 5.22: a) Method A, oven-dried - mixture of spherical, and irregularly shaped aggregated particles; b) Method B, oven-dried - less spherical and non-aggregated; c) Method A, freeze-dried - spherical and less aggregated; d) Method B, freeze-dried - spherical and non-aggregated.

5.2.2.3.3.2. FTIR

The FTIR spectra of OZ and DX exhibited characteristic transmittance as discussed in *sub-section* 4.2.1 (Fig 5.23). TPP spectrum showed characteristic bands at 1214 cm^{-1} (P=O stretching), 1148 cm^{-1} (symmetric and asymmetric stretching of PO_2 group), 1093 cm^{-1} (symmetric and asymmetric stretching of PO_3 group), and 912 cm^{-1} (asymmetric stretching of P-O-P bridge) (Gierszewska-Drużyńska and Ostrowska-Czubenko, 2010). The FTIR peaks of CS at 905 cm^{-1}, 1030 cm^{-1} and 1170 cm^{-1} contributed by presence of D-glucosamine unit which are well preserved in CSTPP microspheres. But, decreased intensity of 1450 cm^{-1} peak of CS in CSTPP microspheres may be contributed by the formation of H-bonding with PO_4 of TPP. Also, band at 1225 cm^{-1}, corresponds to asymmetric stretching vibrations of P=O

groups, indicating formation of ionic crosslinks between TPP ions and NH_3^+ groups of chitosan (Gierszewska-Drużyńska and Ostrowska-Czubenko, 2010; Mi *et al.,* 1999; Pati *et al.,* 2011). The characteristic peaks of drugs were well maintained in the spectra of physical mixture and microspheres, presenting absence of any critical interactions between drugs and polymers. This also supports the encapsulation of drugs within microspheres**.**

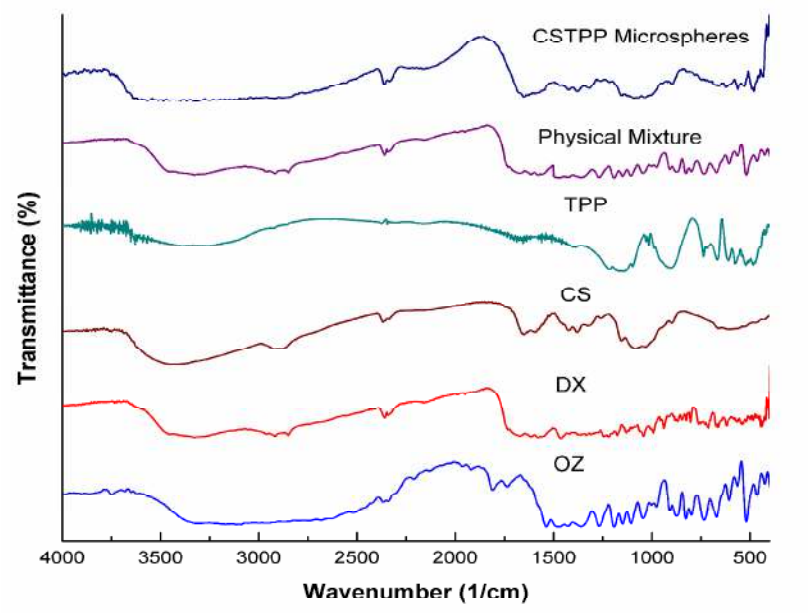

Figure 5.23: FTIR spectra of OZ, DX, CS, TPP, physical mixture and microspheres.

5.2.2.3.3.3. Differential Scanning Calorimetry

In addition to drugs, TPP also exhibited two endothermic peaks attributed to its crystalline nature. Thermal curve of microspheres after heating at increasing temperature does not show any sharp endothermic crystalline peaks of OZ, DX and TPP which reveals amorphous property (Fig. 5.24). Furthermore, disappearance of endothermic peaks of drugs might be reasonable to conversion of crystalline drugs under stress of processing conditions as revealed in *sub-section 5.2.1.6.3.* This also confers to uniform entrapment of both the drugs into microspheres.

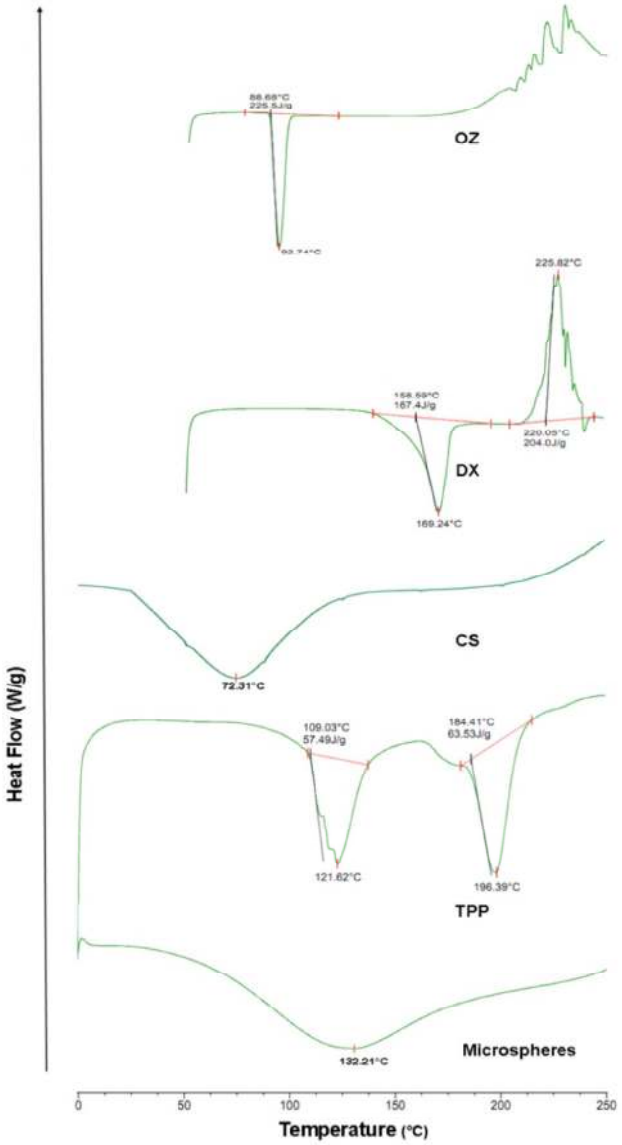

Figure 5.24: DSC thermograms of OZ, DX, CS, TPP and microspheres.

5.2.2.3.3.4. X ray Diffraction

The presence of sharp peaks in the XRD spectra of both drugs indicated their existence as crystalline powder. The sharp intense peaks of TPP also indicated its crystallinity. The crystallinity of drugs and excipients in physical mixtures were well preserved (Fig 5.25). However, microspheres formulated using drugs and excipients showed amorphous behavior. This is in accordance with previous studies which

showed the conversion of crystalline drugs and excipients into amorphous form during formulation of microspheres (Jha *et al.,* 2011; Pandey *et al.,* 2015).

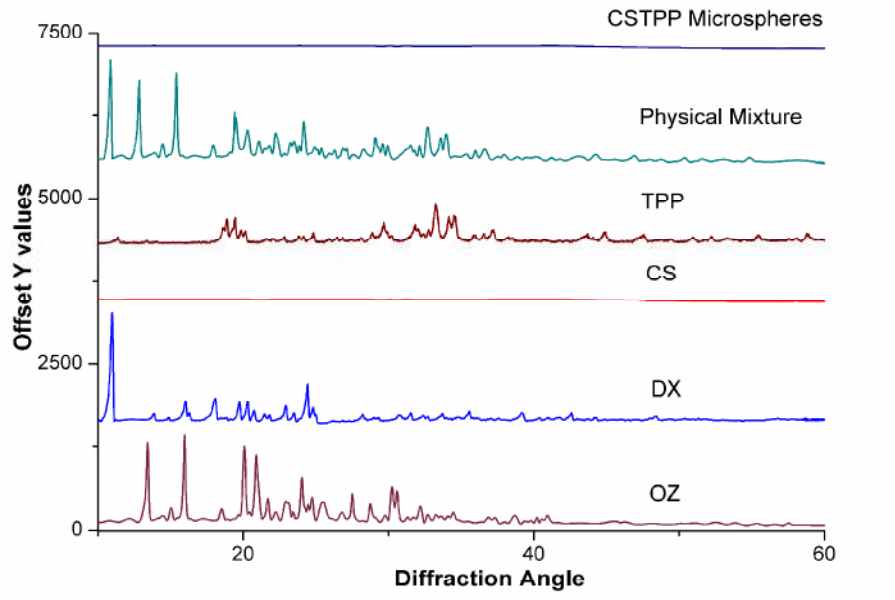

Figure 5.25. XRD patterns of OZ, DX, CS, tripolyphosphate, physical mixture and CSTPP microspheres.

5.2.2.3.4. Mucoadhesivity

Mucoadhesivity is an important parameter for estimation of stay of microspheres at its site of action. Optimized batch showed good mucoadhesivity with 82.51±0.64% microsphere remained attached to mucosal surface after washing. Thus, mucoadhesivity of microspheres maintain required drug concentration by remaining at the site of action. Such high mucoadhesive property of microspheres was contributed by positively charged ammonium groups of CS which has binding affinity with mucosal membranes and supports the intrapocket retention of microspheres as discussed in earlier *sub-section 5.2.1.6.8* (Ma *et al.,* 2014; Songsurang *et al.,* 2011).

5.2.2.3.5. Cytocompatibility study

In SRB assay, non-significant differences were observed in cellular proliferation of L929 or viability and IC_{50} value decreased with increasing incubation time (Fig 5.26 a,b).

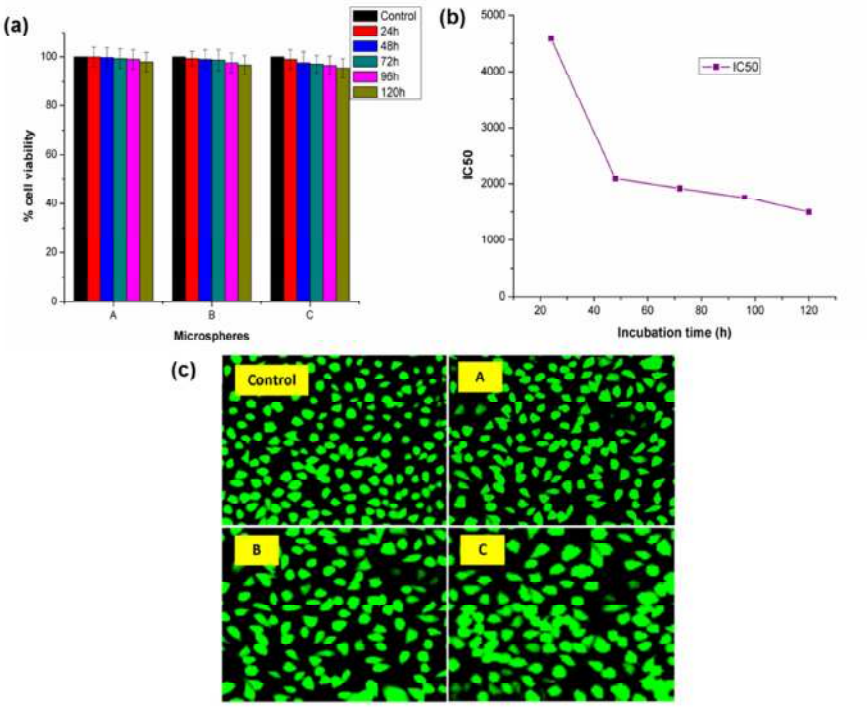

Figure 5.26: (a) Percent cell viabilities of different concentrations of microspheres A (0.01 g/ml), B (0.05 g/ml) and C (0.1 g/ml), incubated in DMEM for 96 h against L929 cell lines. All groups showed non-significant differences in cell viability as compared to control by two-way ANOVA followed by Bonferroni post-tests. Vertical bars represent SEM (n = 6); (b) Incubation time *vs.* IC50 plot; Untreated DMEM media was evaluated as control; (c) Fluorescent microscopic images showing cytocompatibility of various microspheres samples (control, A, B, and C) with L929 cell lines.

The A, B and C concentrations of microspheres expressed more than 98% of cell viability after incubation period. Thus, cytocompatibility of microspheres can be assumed for this period. Seemingly, samples of microspheres (A, B and C) demonstrated generous number of living L929 cells in fluorescent microscope images as compared to control ensuring its safety (Fig. 5.26 c).

5.2.2.3.6. Antimicrobial activity

For success of antimicrobial therapy achievement of concentrations of antibiotics above MIC is prerequisite. In all cases a significant ($p < 0.05$) zone of inhibition had been observed against *S. aureus* and *E. coli* indicating the drug release was above MIC for both organisms as compared to control (Fig 5.27 a and b).

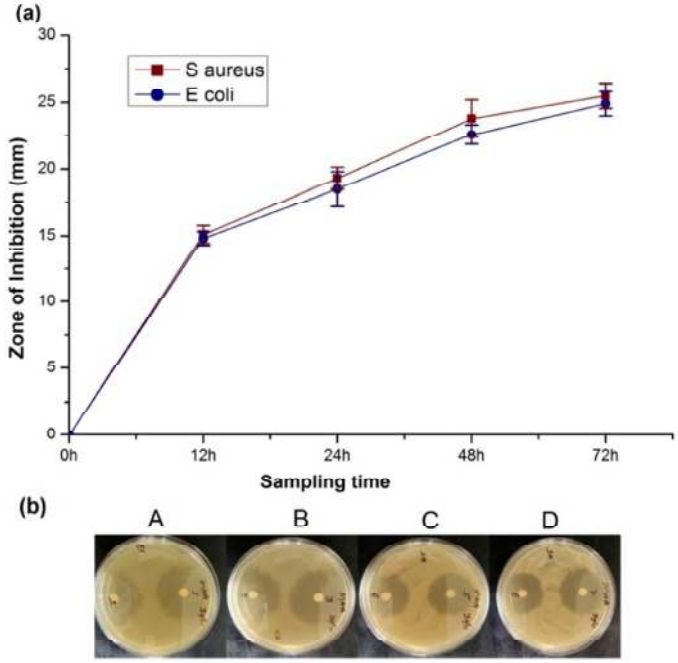

Figure 5.27: (a and b) Antimicrobial activity of *in-vitro* drug release samples at various time interval against *S. aureus* (A and B) and *E. coli* (C and D). Vertical bars represent SD, n = 3. All groups showed significant ($p < 0.001$) zone of inhibition as compared to control (0 h) by two-way ANOVA followed by Bonferroni post-tests.

Furthermore, the sample collected at 12 h with significant zone of inhibition can be correlated to burst effect of drugs desirable for initiation of antimicrobial action. Further, the zone of inhibitions of samples increased with sampling time indicating antimicrobial activity of drugs is dose dependent.

. The outcomes also supposed that *S. aureus* exhibited higher susceptibility than *E. coli* which is well represented by a higher zone of inhibition for *S. aureus*

over *E. coli.* However, the release samples obtained from placebo microspheres (without drug) didn't show any significant antimicrobial activity which could be related to its non-solubility of CS in PBS (Govender *et al.,* 2005). The investigations performed confirmed the effectiveness of fabricated microspheres in periodontal chronic infections.

5.2.2.3.7. *Stability studies*

Stability studies of optimized batch were performed and PS, EE and TDC were determined and compared with fresh samples during storage period. All the physicochemical attributes exhibited non-significant difference ($p > 0.05$) at chosen conditions except at high temperature conditions (Table 5.14). Physical changes like aggregations were observed in the samples stored at high temperature conditions pertaining to absorbance of moisture.

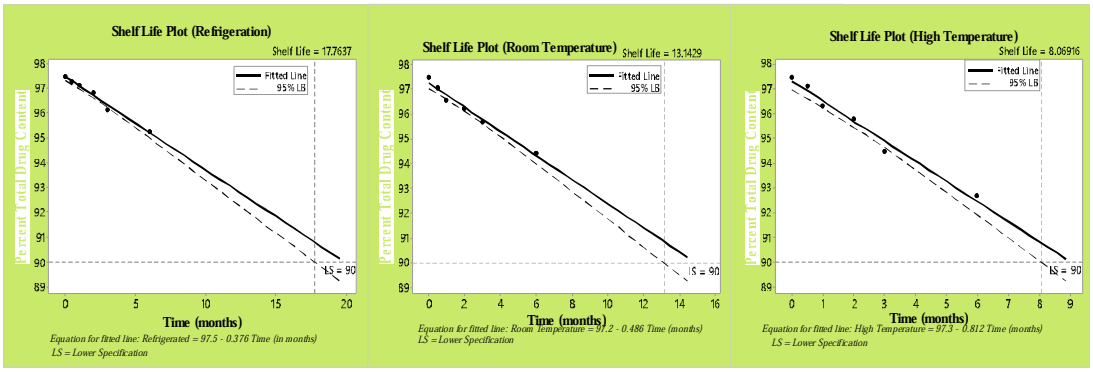

Figure 5.28: Shelf-life plots for CSTPP microspheres at different storage conditions.

The shelf-life of microspheres was 17.76, 13.14 and 8.06 months at refrigeration, room temperature and high temperature storage respectively (Fig 5.28). Thus, the microspheres can be stored and safe for long-term use at refrigerated condition.

Table 5.14: Stability study of CSTPP microspheres after storage for 6 months

Parameters	Fresh Sample	After 6 months		
		Refrigeration	Room Temperature	High Temperature
PS (µm)	168.45±1.76	171.44±2.09	171.12±1.66	186.43±3.86***
EEOZ (%)	85.56±0.89	83.98±0.73	82.88±1	77.37±2.83***
EEDX (%)	91.34±0.65	91.39±1.02	90.33±0.77	87.44±1.67**
BOZ (%)	15.26±1.22	15.67±0.17	16.26±0.54	18.26±0.23***
BDX (%)	12.91±0.67	12.87±0.29	13.31±0.39	15.55±0.48***
TOZ (h)	47.09±0.88	46.79±0.78	45.29±0.17	44.18±1.06**
TDX (h)	67.95±0.33	67.34±1.43	66.53±0.22	64.95±1.33**
TDC (%)	97.48±1.53	95.78±0.67	94.44±1.22	92.67±1.56**

*$p < 0.05$, **$p < 0.01$ and ***$p < 0.001$ All groups are compared with control two-way ANOVA followed by Bonferroni post-tests. Values are mean±SD, n = 3.

5.2.3. Part C

5.2.3.1. *Primary screening of processing factors for crosslinked chitosan microspheres encapsulated with DX using PBFD*

5.2.3.1.1. Experimental design and screening variables

A12 run, 8 factors, 2 levels experimental design were developed by PBFD using Minitab (Table 5.15) and characterized for PS, % EE and $T_{80\%}$. Regression analysis and ANOVA results elaborated the correlation among critical fabrication variables and dependent response variables (Table 5.16).

Table 5.15: A 12 run Plackett-Burman factorial Design of chitosan microspheres

RUN	CS	TCL	CLC	CT	AS	PR	SC	OP	PS* (µm)	EE* (%)	$T_{80\%}$* (days)
1	(-)	(-)	(-)	(-)	(-)	(-)	(-)	(+)	92±8.96	67.22±2.68	6.68±0.26
2	(+)	(+)	(+)	(-)	(+)	(+)	(-)	(-)	110±9.8	88.56±3.52	11.92±0.47
3	(+)	(-)	(+)	(+)	(-)	(+)	(-)	(+)	134±10.04	91.11± 3.64	12.93±0.51
4	(+)	(-)	(+)	(-)	(-)	(-)	(+)	(-)	126±11.62	86.18± 3.44	11.91±0.39
5	(-)	(-)	(-)	(+)	(+)	(+)	(-)	(-)	37±6.09	74.34± 2.96	6.94±0.39
6	(+)	(-)	(-)	(-)	(+)	(+)	(+)	(+)	86±8.75	80.32±3.2	9.88±0.35
7	(+)	(+)	(-)	(+)	(+)	(-)	(+)	(+)	97±9.1	83.14±3.32	10.01±0.40
8	(-)	(+)	(+)	(+)	(-)	(+)	(+)	(+)	74±7.28	79.19± 3.16	8.75± 0.35
9	(+)	(+)	(-)	(+)	(-)	(-)	(-)	(-)	158±11.16	86.23± 1.44	9.81± 0.42
10	(-)	(-)	(+)	(+)	(+)	(-)	(+)	(-)	28±5.46	76.22± 3.04	7.94± 0.35
11	(-)	(+)	(-)	(-)	(-)	(+)	(+)	(-)	77±8.05	66.35± 2.64	6.86± 0.27
12	(-)	(+)	(+)	(-)	(+)	(-)	(-)	(+)	55±6.79	73.78± 2.92	7.54± 0.21

*Values are mean±SD

Pareto analysis disclosed CS, AS, SC and TCL had a significant effect on PS of microspheres. CS, CLC, and CT had a significant effect on % EE of microspheres. Moreover, CS and CLC produced a significant effect on $T_{80\%}$ (Fig 5.29). The CS concentration had the largest effect on all responses. This correlation between variables and responses are well elaborated in surface and contour plots (Fig 5.30). The regression coefficient values (R^2) were above 95% for all the responses, indicating over 95% of the variation in results can be observed and explained by the model. This indicates goodness of fit of the model. Further, the closeness of adjusted R^2 and predicted R^2 values implied adequacy of the regression model (Table 5.16).

The model *p-value* implied that the linear model was significant for all responses ($p < 0.05$). The significance of F and R^2 suggested that there was a good linearity between the predicted and the observed values.

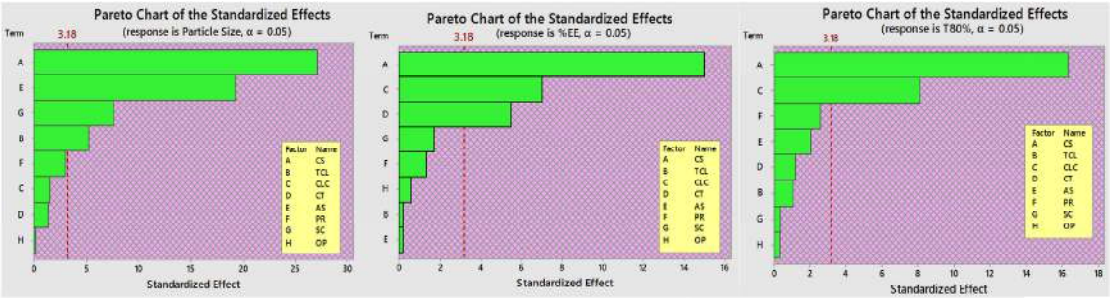

Figure 5.29: Pareto charts representing the effect of formulation variables on responses. The variables beyond reference line (dotted line) are considered significantly important.

Table 5.16: Model Summary and ANOVA results.

Regression parameters	PS (µm)	EE (%)	$T_{80\%}$ (days)
S value	3.69685	1.51841	0.383938
Actual R^2	99.75%	99.04%	99.14%
adjusted R^2	99.10%	96.49%	96.86%
Degrees of freedom	8	8	8
Adjusted SS	16584.0	716.000	51.1337
Adjusted MS	2073.0	89.500	6.3917
F value	151.68	38.82	43.36
p-value	0.001	0.006	0.005

5.2.3.1.2. Dependent response variables

5.2.3.1.2.1. Particle Size

PS = 88.92 + 29.00 CS + 5.67 TCL - 0.833 CLC - 0.0333 CT - 0.04133 AS - 1.583 PR - 8.17 SC - 0.17 OP

The variation in particle sizes was from 37 to 158 µm, indicating a significant effect of formulation variables (Table 5.15).

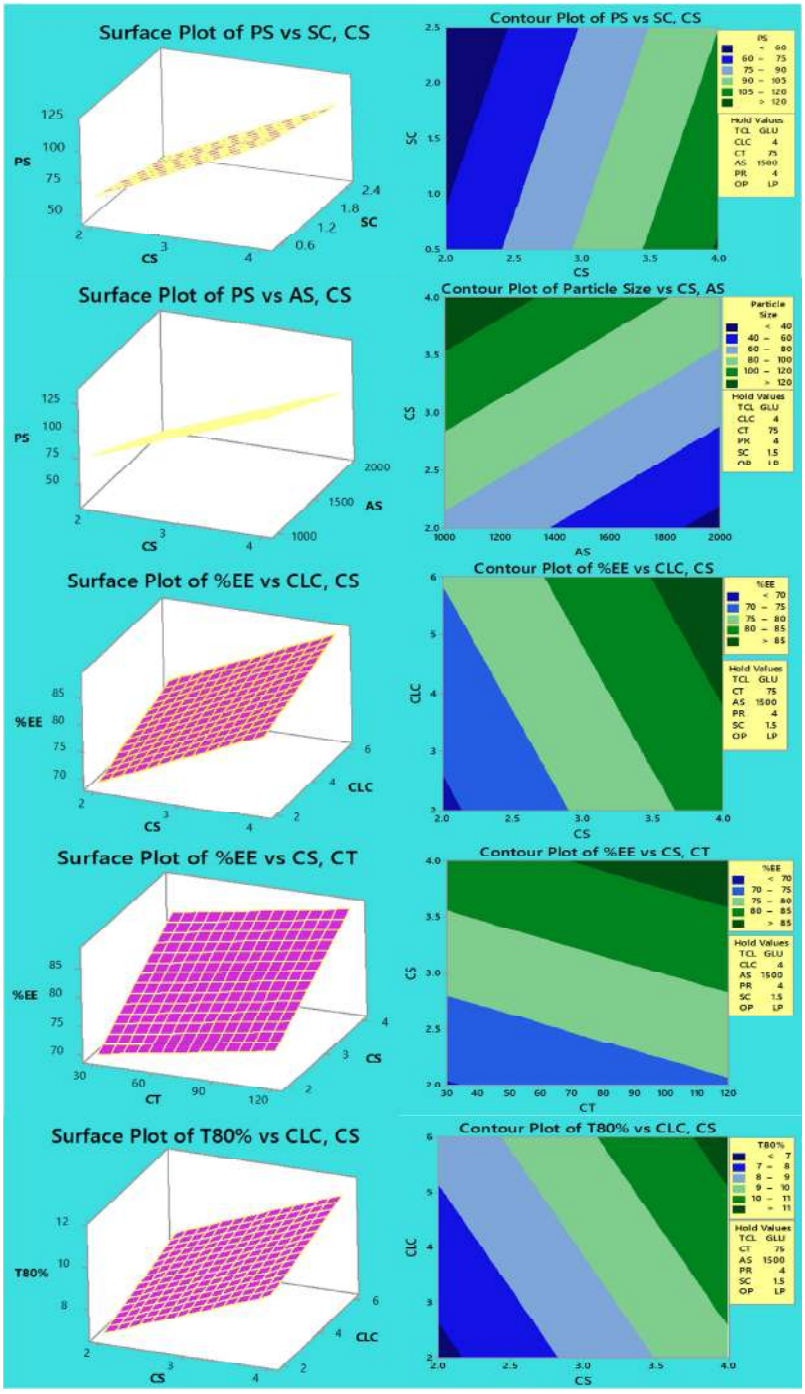

Figure 5.30: Graphs displaying 2D contour and 3D surface plots. The plots show the effect of significant variables on desirable responses.

As far as ANOVA results are concerned for PS, linear model with a *p-value* of 0.001, model F-value of 151.68 and R^2 value of 99.75%, indicated a good correlation between predicted and experimental values. AS, and SC exhibited inverse correlation with PS, while CS and TCL showed a positive correlation as displayed by negative and positive coefficients in the equations respectively. Consequently, increase in AS and SC produced smaller particles owing to increase in force for breakage. Higher CS provided larger particles due to increased viscosity of polymer solution. Moreover, CSV microspheres were found larger than CSG microspheres.

5.2.3.1.2.2. Entrapment efficiency

% EE = 49.35 + 6.583 CS + 0.083 TCL + 1.542 CLC + 0.05370 CT - 0.000167 AS + 0.292 PR - 0.750 SC + 0.250 OP

The % EE for crosslinked microspheres were found in a very wide range of 66 to 91%. Such variability was attributed to the presence of two types of crosslinkers *viz.* VAN and GLU. Linear polynomial equations retained significant terms without interactions. As per Pareto analysis and linear equations, CS, CLC, and CT have a positive influence on % EE (Fig. 5.29). These screened variables tend to enhance % EE at their high level. This effect was observed, as an increase in CS, CLC and CT contribute towards increment of crosslinked networks in microspheres bringing maximal entrapment of DX. These trends in variations are well depicted in response and contour plot (Fig 5.30).

5.2.3.1.2.3. $T_{80\%}$

$T_{80\%}$ = 2.31 + 1.508 CS + 0.105 TCL + 0.398 CLC + 0.01304 CT - 0.000177 AS + 0.127 PR - 0.293 SC + 0.045 OP

$T_{80\%}$ was estimated from *in-vitro* drug release profiles of all microspheres. The range of responses for $T_{80\%}$ varied from 6.68 to 12.93 days. ANOVA results with F-value of 43.36 and *p-value* of 0.005 suggested well elaborations of expected responses by the model. CS and CLC had significantly and positively affected $T_{80\%}$ (Fig. 5.29). As discussed earlier, the rise in CS and CLC improved drug entrapment

by increasing crosslinking matrix. Consequently, this increase in crosslinking network within microspheres reduces the drug release, hence increases the time required for 80% of drug release ($T_{80\%}$) (Fig 5.30).

5.2.3.1.3. Optimization and validation

The final optimized formulation was produced based on combined effect of all the variables with the composite desirability of 0.7034 by fixing constraints for independent variables (Table 5.17).

Table 5.17. Theoretical and experimental values of responses and their validation.

Variables	Optimized Formulation	Desirability
CS	3.5%	0.7034
TCL	Vanillin	
CLC	6%	
CT	120 min	
AS	2000 rpm	
PR	1:4	
SC	2.5%	
OP	Soyabean oil	

Responses	Target	Predicted Value	Observed Value (mean±SD, n = 3)	% Bias
PS (µm)	Minimize	77.5	75.45±3.56	2.645
EE (%)	Maximize	87.37	88.87±1.22	-1.722
$T_{80\%}$ (days)	Maximize	10.78	10.41±0.42	3.432

For optimization, the target applied was lower PS, higher % EE, and higher $T_{80\%}$. The optimized batch was obtained at following conditions: CS (3.5%), TCL (VAN), CLC (6%), CT (120 min), AS (2000 rpm), PR (1:4), SC (2.5%) and OP (Soyabean oil). The desirable responses such as PS, % EE, and $T_{80\%}$ for practically formulated batches were found to be 75.45 µm, 88.87% and 10.41 days respectively (Table 5.17). The experimentally obtained values presented a sound agreement with

acceptable percentage bias (< 15%) which justifies good fit of the model. Thus, VAN was chosen as optimized crosslinker.

5.2.3.1.4. Evaluation of optimized batch

The optimized CSV microspheres were evaluated for following parameters. Further, similar CSG microspheres were also formulated for comparative study with optimized CSV microspheres.

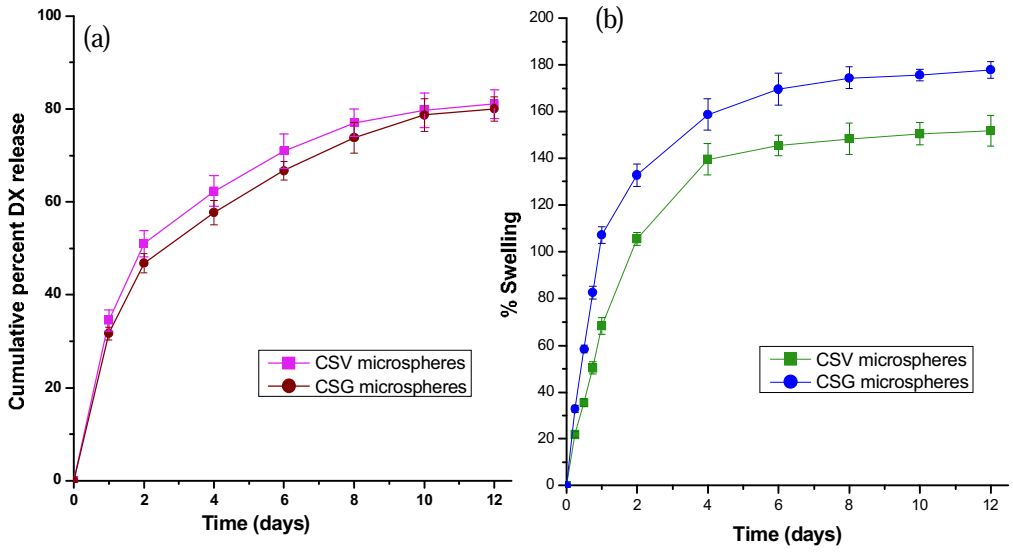

Figure 5.31: Comparative (a) *In-vitro* doxycycline hyclate release and (b) *In-vitro* swelling of optimized CSV and CSG microspheres. Vertical bars represent SD.

5.2.3.1.4.1. Drug release kinetics

The comparative release profiles of CSV and CSG microspheres are shown in Fig. 5.31a. The drug release profile exhibited a biphasic pattern of drug release. Burst release constituted the first phase and the second phase was the slow drug release phase. There are many concepts behind burst release behavior; a) due to the presence of free drug on microspheres surface, b) initial rapid swelling of microspheres due to fast ingression of dissolution media. After swelling equilibrium was attained, the drug release was slowed down. The drug release was controlled and prolonged till 12 days

after which no significant change in drug release was observed. CSG exhibited the lesser burst and slower release than CSV ascribed to strong crosslinking networks.

Further, this result is also supported by lower DX diffusion coefficient values of CSG (8.49×10^{-4}) than CSV (2.48×10^{-4}) microspheres. The diffusion coefficient is directly proportional to the rate of drug released. Drug release mechanism was determined by fitting the release data into various kinetic equations. Based on R^2 values the release followed Higuchian kinetics or matrix controlled kinetics (Table 5.18). Further, from Korsmeyer-Peppas model drug release mechanism was further elaborated. The 'n' values were more than 0.43, confirming non-Fickian diffusion mechanism of drug release. The microspheres followed diffusion as well as swelling controlled drug release from matrix irrespective of the type of crosslinker.

Table 5.18. Comparative drug release kinetics of CSV and CSG microspheres.

Batch	Zero-order Kinetics		First-order Kinetics		Higuchi-Kinetics		Hixson-Crowell Kinetics		Korsmeyer-Peppas		
	K (mgh/ml)	R^2	K (h^{-1})	R^2	K ($h^{-1/2}$)	R^2	K ($h^{-1/3}$)	R^2	K (h^{-n})	R^2	n
CSV	2.122	0.850	0.144	0.710	35.05	0.933	0.274	0.899	1.439	0.919	0.656
CSG	11.205	0.860	0.143	0.722	32.33	0.940	0.244	0.902	1.335	0.926	0.649
Diffusion Coefficient (cm^2/sec)											
CSV			8.49×10^{-4}				CSG		2.48×10^{-4}		

*Values are mean±SD

5.2.3.1.4.2. NMR

The crosslinking of VAN and CS in optimized CSV microspheres were confirmed by ^{1}H-NMR spectra (Fig. 5.32). The characteristic peaks for CS are observed at $\delta = 1.22$ (-$CH_2CH_2CH_2$-, alkane), $\delta = 1.96$ ($NHCOCH_3$), 2.25 and 2.6 (CH_2-CONH, acetyl protons of chitosan), $\delta = 2.5$ (CH-N) (proton present at chitosan ring, to which –NH_2 group is attached.), $\delta = 3.5$-3.81 (CH_2 bridge protons/chitosan

glucopyranose ring protons), $\delta = 4.5$ (alkyl amine chitosan anomeric proton), and $\delta = 5.10$ ppm (O-CH-O).

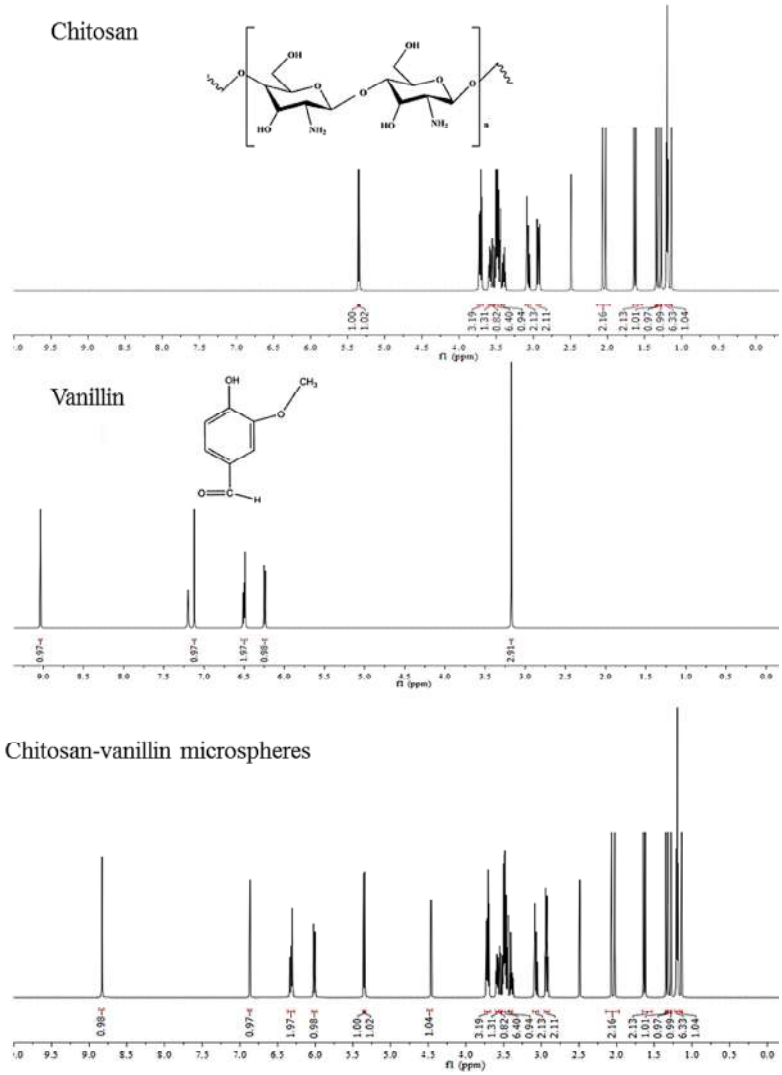

Figure 5.32: ^{1}H NMR of chitosan, vanillin and placebo chitosan-vanillin microspheres

VAN exhibited $\delta = 3.8$ (for -OCH3), $\delta = 6.7$-7.4 (aromatic H of VAN ring), $\delta = 6.9$ (aromatic CH- attached to OH) and $\delta = 9.7$ ppm (aldehyde), ^{1}H-NMR spectra of optimized placebo CSV microspheres (without drugs) showed intense peaks in the aliphatic region (1 - 5 ppm) due to presence of hydrogens of chitosan and VAN

(phenol and methoxy hydrogens). In the aromatic region weak peaks are present, due to the aromatic hydrogens of VAN ring (6.7 -7.2 ppm). The shifting of CHO peak (9.4 ppm) to CHN (8.8 ppm) confirms Schiff-base formation between CS and VAN in placebo CSV microspheres (dos Santos *et al.,* 2005).

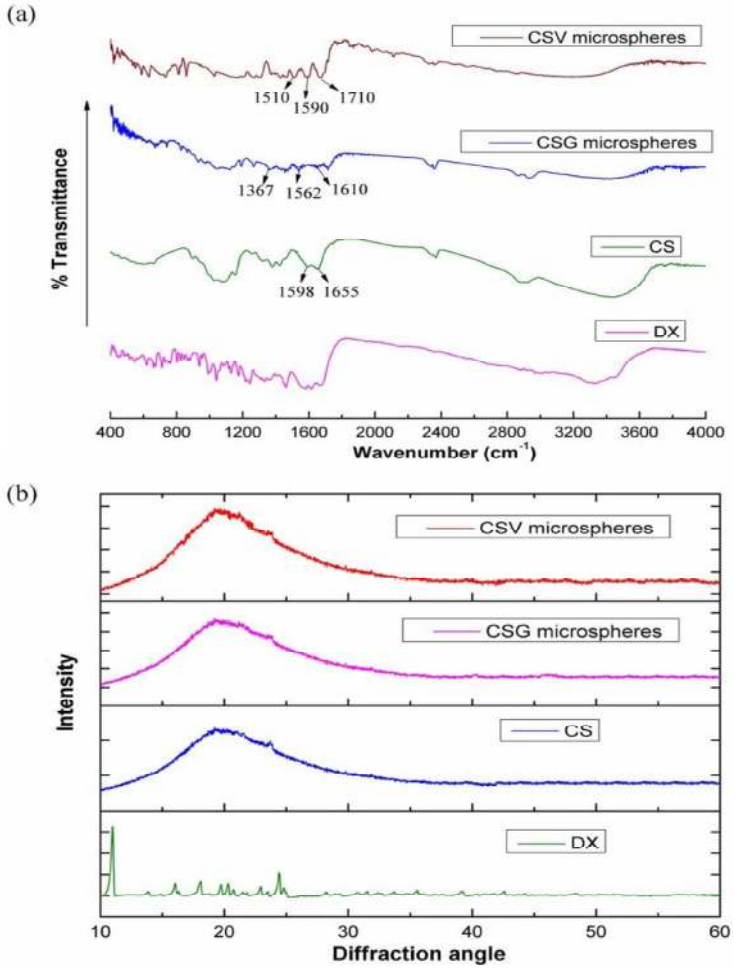

Fig 5.33: (a) Infrared spectra and (b) X-ray Diffraction graphs of DX, CS, CSG microspheres and CSV microspheres.

5.2.3.1.4.3. FTIR

The characteristic functional groups present in CS, VAN and GLU are responsible for their reactivity and were characterized by using FTIR (Fig 5.32a). The CSV microspheres showed distinguishing absorption bands of VAN at 1510 (benzene ring) and peculiar absorption band at 1710 cm^{-1} represents the Schiff base formation

(C=N) between CS and VAN as revealed by NMR studies (Yang *et al.,* 2014). Moreover, the –OH peaks of CS at 3450 is shifted to 3420 cm^{-1} with reduced intensity, which could be attributed to H-bonding interactions between CS and VAN (Fig 5.33a).

In CSG microspheres, the typical absorption peaks at 1400 cm^{-1} (C-H bending) and 1350 cm^{-1} (O-H bending) belonged to CS. Further, absorption at 1610 cm^{-1}epitomizes formation of imine bond (C=N) between –CHO groups of the condensation product of GLU and $–NH_2$ groups of CS by Schiff base reaction (Fig 5. 33a). This interaction between GLU and CS is well established since decades (Jameela and Jayakrishnan, 1995; Khan *et al.,* 2016). Besides, the peak at 1562 cm^{-1} is reflective of C=C bond formation as a result of condensation and dehydration of GLU (Khan *et al.,* 2015). The unreacted free amino groups are observed at 3300 and 3367 cm^{-1} in both microspheres (Hu *et al.,* 2013). In addition the drugs and polymer peaks were well preserved in both microspheres.

5.2.3.1.4.4. XRD

The diffraction plots for DX, CS and crosslinked microspheres are depicted in Fig 5.33b. Likewise, the crosslinked microspheres displayed amorphous nature with the absence of all sharp peaks related to DX. The absence of sharp peaks of the drug indicates loss of crystalline nature of drug during manufacturing of microspheres and uniform dispersion of drug into microspheres (Hu *et al.,* 2013). Additionally, both CSV and CSG microspheres illustrated diffraction pattern similar to CS, confirming their amorphous character.

5.2.3.1.4.5. Morphology

SEM assessed the shape and surface morphology of microspheres. Noteworthy differences in morphology were observed between CSV and CSG microspheres (Fig. 5.34). The shapes of VAN microspheres varied from spherical to elongate with a smooth surface and some depressions on the surface formed during drying (Fig. 5.33 a, b).

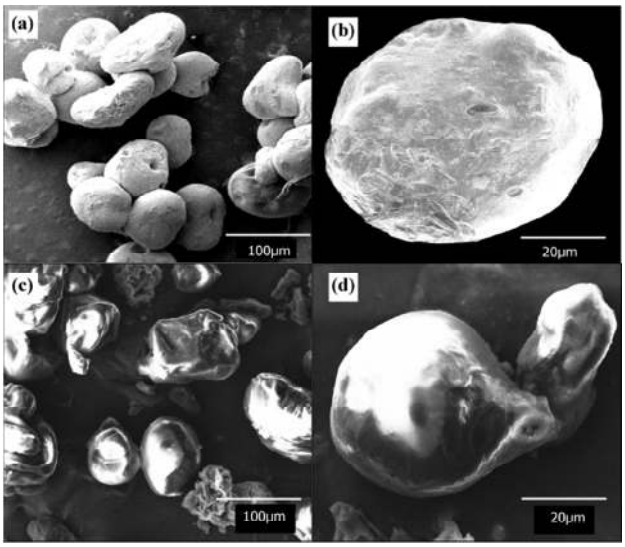

Figure 5.34: SEM images; (a) Cluster and (b) Single CSV microspheres ;(c) bunch and (d) single CSG microspheres.

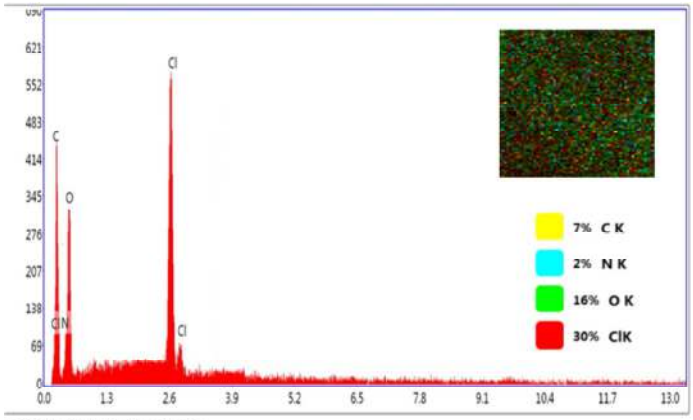

Element	Weight %	Atomic %
C	32.75	40.8
N	10.22	10.92
O	47.21	44.15
Cl	9.81	4.14

Figure 5.35: EDXA spectra showing elemental composition of optimized CSV microspheres.

Although, the particles of CSG microspheres observed were smaller in size but were of irregular shapes (Fig. 5.34c,d). Overall, the crosslinked microspheres exhibited smooth surface morphology in a similar manner as reported by Gupta and

Jabrail, (2007) (Gupta and Jabrail, 2007). Further, EDXA plot indicate uniform dispersion of all the elements belonging to drugs and excipients and elemental composition of optimized CSV microspheres (Fig. 5.35).

5.2.3.1.4.6. Swelling studies

CS is a hydrophilic polymer as it contains –OH and $–NH_2$ groups. Nevertheless, the hydrophilic behavior of CS gets modified after crosslinking interactions. Previous researchers have elaborated that crosslinked chitosan matrix are more rigid than pure CS matrices and hence, show lower swelling. An optimum swelling is desirable for controlled drug release and prevention of oozing out of microspheres from the pocket (Khan *et al.,* 2015).

The degree of swelling of CSV and CSG microspheres were compared (Fig 5.31b). The microspheres showed biphasic type swelling behavior constituted by rapid swelling and slow swelling phase. CSV microspheres showed rapid swelling for about four days followed by slow or constant swelling phase whereas CSG microspheres exhibited rapid swelling for about six days followed by a slow phase. Thus, lower swelling of CSV is attributed to its high hydrophobicity imparted by aromatic group. The conjugative effect of benzene ring increases the hydrophobic property of CSV microspheres and lowers its swelling (Gupta and Jabrail, 2007). In comparison, CSG microspheres are hydrophilic and showed higher swelling. Therefore, crosslinking of CS with aromatic VAN increases its hydrophobicity than with hydrocarbon chain based GLU (Zou *et al.,* 2015). The lower degree of swelling of CSV indicates its utility in controlled drug release

5.2.3.1.4.7. Degree of crosslinking

The basic principle behind Ninhydrin assay is the conversion of yellow Ninhydrin dye into the purple color compound on reacting with the free amino acid group. The optical density of purple color determines the free amino acid groups. The presence of free amino groups was determined for CSG and CSV microspheres to estimate the extent of crosslinking. The degree of crosslinking is also responsible for

other physicochemical properties of microspheres like swelling, drug release, mucoadhesion, *etc*. The degree of crosslinking for CSV microspheres was found to be 54.28%, and for CSG microspheres was 67.51%. The lower degree of crosslinking of CSV than CSG microspheres may be produced by conjugative effects of benzene ring present in VAN (Zou *et al.,* 2015). A Higher degree of crosslinking offers formation of more crosslinked networks within microspheres and controls the drug release but lowers its mucoadhesion property as discussed in next *section*.

5.2.3.1.4.8. *Mucoadhesion studies*

CS is a mucoadhesive polymer carrying positively charged amino groups which are accountable for reacting with negatively charged mucous membranes of gums. The mucoadhesion of CSV and CSG microspheres were found to be 76.32 and 65.94% respectively, indicating a higher percentage of CSV microspheres retention by mucous membranes. This observation may also be because of lower degree of crosslinking of CSV microspheres and higher availability of free amino acid groups on the surface of microspheres for reacting with mucous membranes (Genta *et al.,* 1998).

5.2.3.1.4.9. Cytocompatibility study

SRB is a negatively charged bright pink aminoxanthine dye taken by basic amino acids in the TCA fixed cells, and colorimetric evaluation provides an estimate of total protein mass which is directly proportional to cell number. The greater the number of cells, the greater amount of dye is taken up and, after fixing, when the cells are lysed, the released dye will give a more intense color and greater absorbance (Houghton *et al.,* 2007). The SRB assay was used to evaluate the effects of drugs on the metabolic activity of mice fibroblast cells L929. Microspheres samples (CSV and CSG) showed cytocompatibility with L929 cell lines (Fig 5.36 a&b), and high cell viability was observed in CSV samples (A, B and C) than CSG samples. The CSV samples showed the non-significant difference ($p < 0.05$) in percent viability till 7^{th} day as compared to control indicating their safety for use in the periodontal cavity. However, CSG microspheres demonstrated biocompatibility, it has exhibited lower

IC_{50} values as compared to CSV microspheres. Glutaraldehyde is in general considered as toxic beyond certain concentration (Takigawa and Endo, 2006). Thus, VAN is FDA approved and can be used as a safe substitute for GLU for formation of prolonged release crosslinked chitosan microspheres.

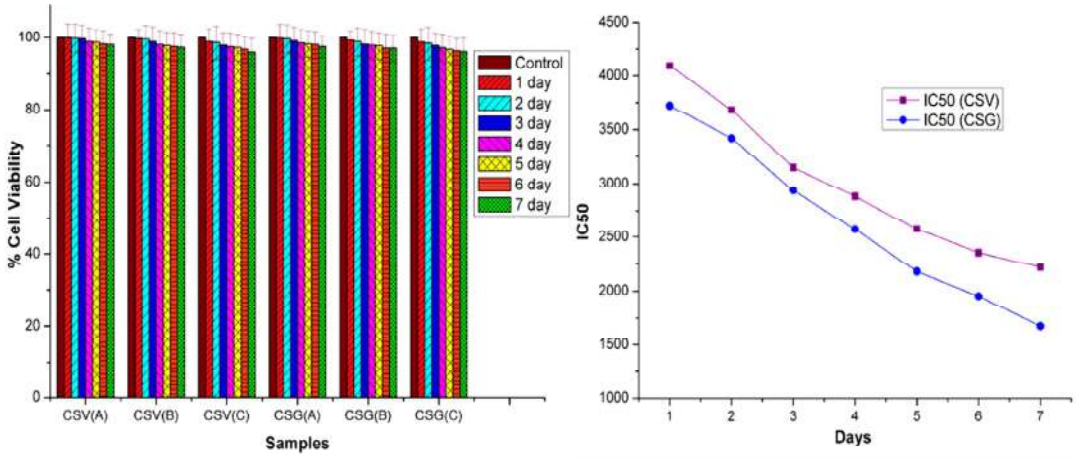

Figure 5.36: Comparative cytocompatibility studies of CSV and CSG microspheres and IC50 values calculation. All groups showed non-significant differences in cell viability as compared to control by two-way ANOVA followed by Bonferroni post-tests. Vertical bars represent SEM (n = 6).

5.2.3.1.4.10. Antimicrobial activity

Earlier studies had reported the presence of *S. aureus* in the oral microflora of Periodontics patients (Do *et al.,* 2014). Optimized CSV microspheres having higher biocompatibility were selected for evaluation of antimicrobial potency. Drug release samples collected on 1 day and 7th day after dissolution studies were evaluated for their antimicrobial potency against *S. aureus* and *E. coli* by determining zone of inhibition (Fig 5.37b). In all cases, significant ($p < 0.05$) zone of inhibition had been observed indicating activeness of samples for both organisms. Further, the zone of inhibitions of samples increased with time of sampling due to higher antibiotic concentration, indicating antimicrobial activity of drugs is dose dependent. Further, little antimicrobial activity may be attributed CS and VAN complexes as reported in earlier studies (Stroescu *et al.,* 2013). Also, the outcomes of the study reveal the higher activity of samples for *S. aureus* than *E. coli*. The investigations performed

confirmed the effectiveness of fabricated microspheres in chronic infections such as periodontitis.

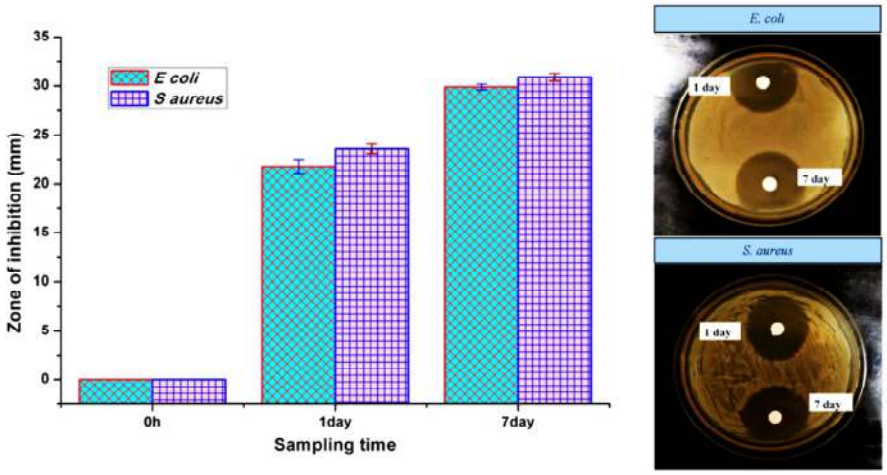

Figure 5.37: Antimicrobial activity of optimized CSV microspheres against *E. coli* and *S. aureus*. Vertical bars represent mean±SD, n = 3. All groups showed significant ($p < 0.001$) zone of inhibition as compared to control (0 h) by two-way ANOVA followed by Bonferroni post-tests.

5.2.3.1.4.11. Stability study

Stability study was performed for 6 months by determining changes in PS, EE and $T_{80\%}$ of the optimized CSV batch. It was observed that on storage at low and room temperature changes in PS, EE and $T_{80\%}$ was non-significant ($p > 0.05$). On the other hand, storage at high-temperature conditions had produced significant changes in PS, EE and $T_{80\%}$ (Fig 5.38a). Assay of DX content (TDC) in optimized microspheres was executed, and shelf-life (t) at different storage conditions were calculated using following software generated equations:

Low temperature; TDC = 99.8-0.389t

Room temperature; TDC = 99.9-0.456t

High temperature; TDC = 99.8-0.864t

The negative sign of coefficient shows the drug content of microspheres decreases with increase in time of storage, which may be caused by degradation of doxycycline hyclate during storage. The maximum shelf-life was estimated as 19.19

months for refrigerated samples, followed by samples stored at room temperature (17.64 months) and then high-temperature conditions (9.92 months) (Fig 5.38b). This result may be credited to enhanced drug degradation at high temperature conditions. Therefore, it is suggested to store microsphere should be stored at low or room temperature conditions for prolonged use.

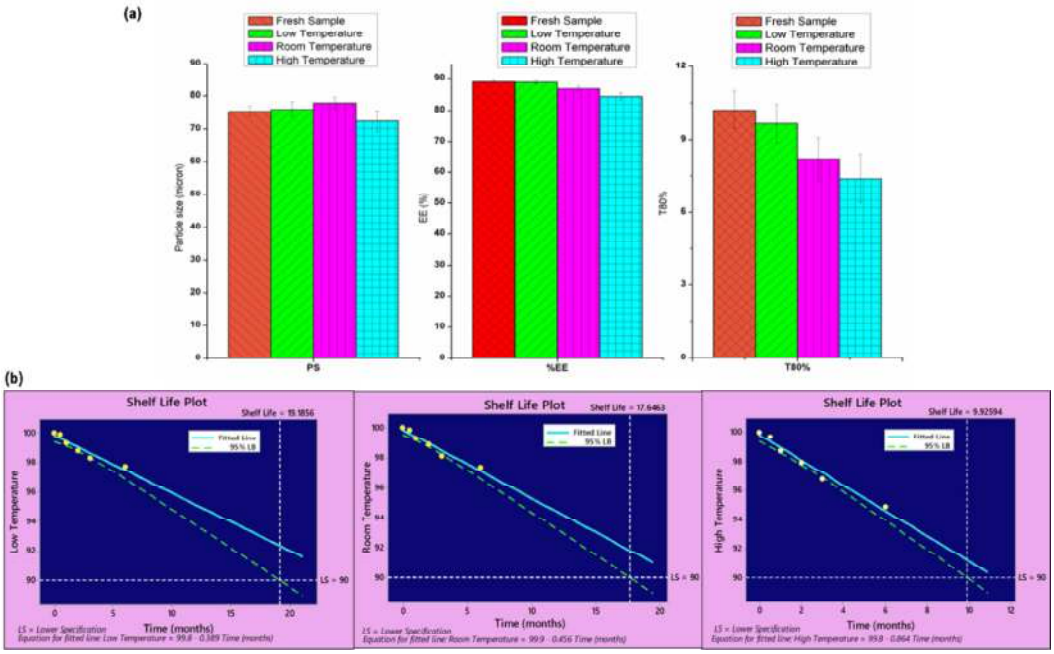

Figure 5.38: (a and b) Stability studies and shelf-life of optimized CSV microspheres. Vertical bars in (a) represent SD, n=3.

5.2.3.2. Final optimization of crosslinked chitosan-vanillin (CS-VAN) microspheres based on significant formulation variables using Box-Behnken Design (BBED)

5.2.3.2.1. Experimental design and optimization of microspheres

The variations in obtained responses were analyzed by ANOVA and regression analysis to study the effect of various fabrication variables on the dependent variable and whether the variations occurred due to processing conditions or by chance. The responses obtained are given in Table 5.19.

5.2.3.2.1.1. Particle Size

The mean PS of microspheres ranged between 22 to 126 µm (Table 5.19). CS and SC had significant ($p < 0.05$) positive and negative effects on PS as revealed by positive and negative coefficients, respectively. This relation is well explained by following coded polynomial equation:

$$PS = +69.00+37.00CS+0.12VC-14.38SC-4.75CS*VC+2.75CS*SC+4.50VC*SC +7.00CS^2+1.25VC^2+0.75SC^2$$

The Model F-value of 291.57 and *p-value* < 0.05 implied that the model was significant. The "Lack of Fit F-value" of 7.58 was non-significant (Table 5.20). The "Predicted R^2" of 0.9717 was in reasonable agreement with the "Adjusted R^2" of 0.9947 suggesting adequacy of model. "Adequate Precision" measures the signal to noise ratio and value of 56.56 (> 4) indicates adequate signal. It was observed that increase in SC had remarkably decreased mean PS, due to stabilization of emulsion droplets. Also, it has been observed that mean PS increased rapidly with increment in CS concentration. Higher CS concentration leads to higher viscosity of dispersed phase thus the particle size increases. These effects are well demonstrated by 2D and 3D surface plots (Fig 5.39 and 5.40).

Table 5.19: Box-Behnken Experimental Design with obtained responses.

Std run	CS (%)	VC (%)	SC (%)	PS (µm)	EEOZ (%)	EEDX (%)	TOZ (days)	TDX (days)	M (%)
1	(-)	(-)	(0)	34±2.72	66.82±3.11	69.77±2.13	6.67±0.301	6.53±0.29	64.44±2.9
2	(+)	(-)	(0)	117±9.36	80.56±2.62	82.13± 3.69	10.56±0.47	10.42±0.46	88.61±3.987
3	(-)	(+)	(0)	47±3.76	75.31±1.38	76.37±3.43	6.82±0.307	6.73±0.37	58.15±2.617
4	(+)	(+)	(0)	111±.88	88.52±1.98	91.61±4.12	12.03±0.54	11.88±0.535	81.34±3.66
5	(-)	(0)	(-)	57±4.56	72.21±3.24	74.82±1.36	7.45±0.34	7.56±0.34	61.91±2.78
6	(+)	(0)	(-)	126±10.08	87.08±3.91	89.17±4.01	11.85±0.53	11.74±0.52	85.53±3.84
7	(-)	(0)	(+)	22±1.76	71.19±2.21	72.21±3.24	7.21±0.32	7.17±0.32	63.63±2.86
8	(+)	(0)	(+)	102±8.16	85.77±3.86	88.1±1.96	11.72±0.52	11.64±0.52	86.18±4.03
9	(0)	(-)	(-)	91±7.28	77.46±3.48	78.41±3.52	7.53±0.33	7.41±0.33	76.42±3.43
10	(0)	(+)	(-)	79±6.32	82.01±3.69	83.18±2.74	10.14± 0.45	10.01±0.45	68.81±1.09
11	(0)	(-)	(+)	54±4.32	74.11±2.33	76.45±3.44	6.81±0.31	6.78±0.30	76.67±3.45
12	(0)	(+)	(+)	60±4.8	82.85± 3.73	84.21±3.78	9.71± 0.43	9.59±0.43	72.48±2.26
13	(0)	(0)	(0)	68±5.44	81.91±3.68	82.12±1.69	8.53±0.38	8.45±0.38	73.23±3.29
14	(0)	(0)	(0)	69±5.52	81.22±2.65	83.52±3.75	8.47±0.31	8.38±0.377	74.71±3.36
15	(0)	(0)	(0)	70±5.6	81.04±0.64	82.34±2.71	8.55±0.34	8.46±0.381	74.88±1.37

*values are mean±SD

Table 5.20: Model Summary and ANOVA results

Responses	R^2	Adjusted R^2	Predicted R^2	Adequate Precision	F value	*p-value* Prob > F
PS (µm)	0.998	0.9947	0.9717	56.562	7.58	< 0.0001
EEOZ (%)	0.995	0.9873	0.938	37.638	3.21	< 0.0001
EEDX (%)	0.995	0.9873	0.9393	37.638	2.86	< 0.0001
TDX (days)	0.990	0.9876	0.9801	59.58	7.94	< 0.0001
TOZ (days)	0.989	0.9866	0.9785	57.14	6.16	< 0.0001
% M	0.997	0.9941	0.9852	51.36	0.7981	< 0.0001

The variations in obtained responses were analyzed by ANOVA and regression analysis to study the effect of various fabrication variables on the dependent variable and whether the variations occurred due to processing conditions or by chance.

5.2.3.2.1.2. Entrapment Efficiency

The EE of all formulations was in the range of 66.82 to 88.52% (EEOZ) and 69.77 to 91.61% (EEDX) (Table 5.19). The significant variables affecting EE positively were CS and VAN concentration ($p < 0.05$). SC had shown non-significant effect on EE. The effect can be described by following quadratic equations:

$$EEOZ = 81.39 + 7.05CS + 3.72VC - 0.61SC - 0.13CS*VC - 0.073CS*SC + 1.05VC*SC - 1.82CS^2 - 1.77VC^2 - 0.51SC^2$$

$$EEDX = 83.92 + 7.02CS + 3.72VC - 0.63SC - 0.14CS*VC - 0.13CS*SC + 1.04VC*SC - 1.84CS^2 - 1.76VC^2 - 0.54SC^2$$

The Model F-values implied that model was significant ($p < 0.05$) for both EEOZ and EEDX. The "Predicted $R^{2"}$ was in reasonable agreement with the "Adjusted $R^{2"}$. "Adequate Precision" was greater than four is desirable for indicating adequate signal. The increment in entrapment of drugs was observed with increased in both CS and VAN concentration as revealed by positive coefficients in the

equation. This may be due to the availability of a large amount of polymer for the entrapment of drugs. Further, increase in crosslinker VAN decreases the drug loss during processing of microspheres.

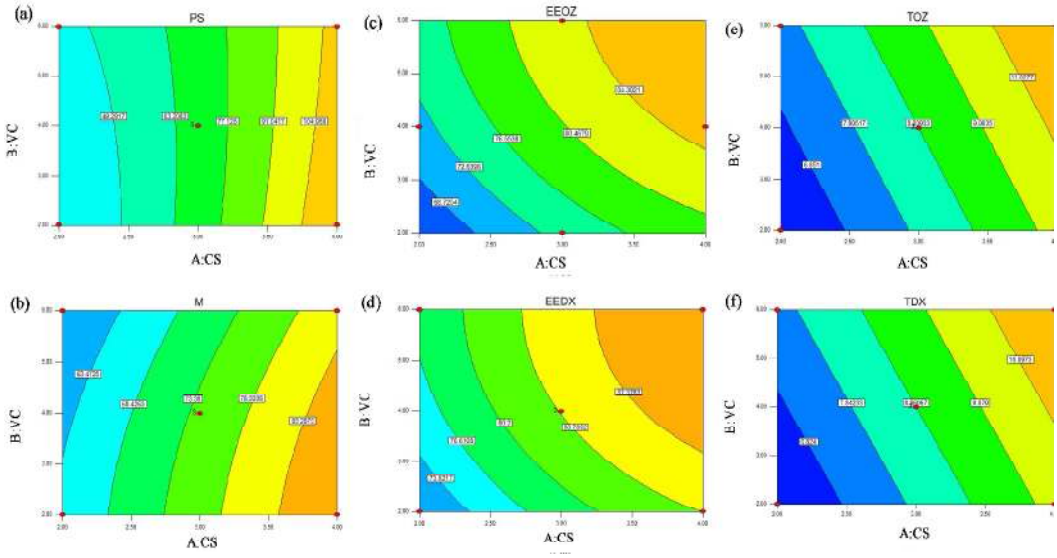

Figure 5.39: 2D surface plots illustrating the effect of independent variables on responses associated with chitosan-VAN microspheres.

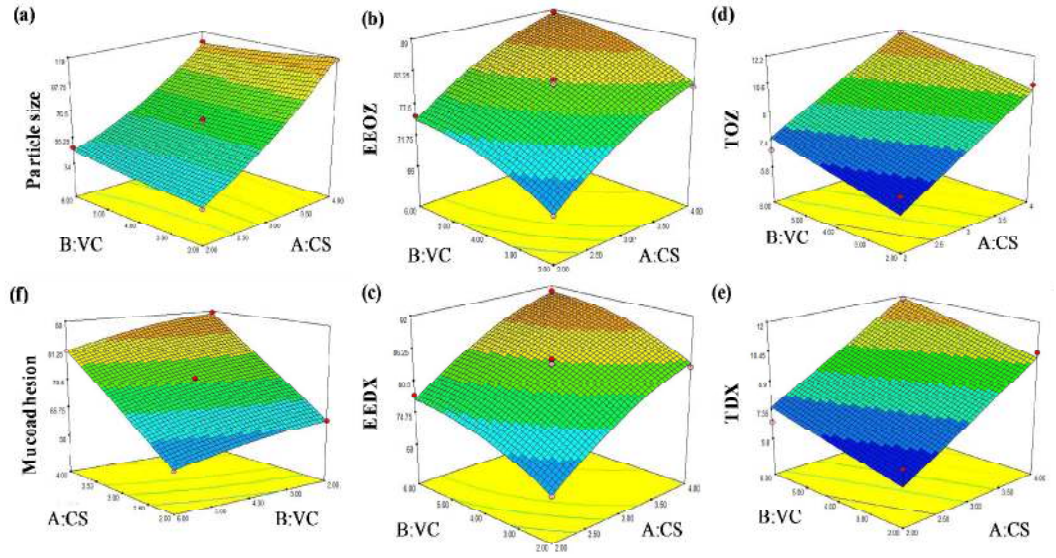

Figure 5.40: 3D surface plots illustrating the effect of independent variables on responses associated with chitosan-VAN microspheres.

5.2.3.2.1.3. Time for 80% drug release

Final linear equation in terms of coded variables for TOZ and TDX:

$TOZ = 8.08 + 2.9CS + 1.17VC - 0.18SC$

$TDX = 8.63 + 2.91CS + 1.17VC - 0.18SC$

The Model F-values showed significant model with $p < 0.05$. The significant variables *viz.* CS and VAN concentration (VC) with positive coefficients affected $T_{80\%}$ positively (A and B) ($p < 0.05$) (Table 5.20). The "Lack of Fit F-value" of 6.16 (TOZ) and 7.94 (TDX) intimated non-significant Lack of Fit relative to the pure-error. The "Predicted R^2" was in reasonable agreement with the "Adjusted R^2"in both cases. Adequate Precision ratio indicated an adequate signal. Higher amount of CS and VAN in microspheres matrix increases the barrier for drug diffusion and drug release, the elevated $T_{80\%}$ was observed with both drugs.

5.2.3.2.1.4. Percent in-vitro mucoadhesion

Mucoadhesion is a critical step in localized periodontal drug delivery for retention of drugs at site of action. Final equation in terms of coded variables for percentage mucoadhesion of microspheres (%M);

$M = 74.27 + 11.69\ CS - 3.17\ VC + 0.79\ SC - 0.24\ CS*VC - 0.27\ CS*SC + 0.86\ VC*SC - 0.21\ CS^2 - 0.93\ VC^2 + 0.25\ SC^2$

The Model F-value of 262.30 advocated significant model ($p < 0.05$) (Table 5.20). The Lack of Fit of 0.35 suggested the "Lack of Fit" was not significant. "Predicted R^2" of 0.9852 was in reasonable agreement with the "Adjusted R^2" of 0.9941. "Adequate Precision" ratio of 51.36 provided an adequate signal. The positive coefficients of CS and SC reveals their direct relation with % M. On the contrary, VAN had an inverse relation with mucoadhesion. The increment in CS concentration improves the number of free amino groups and offers binding affinity to negatively charged mucin. On the other hand, increased SC enhances the mucoadhesion by reducing PS and increasing surface area available for

mucoadhesion. However, raising VAN concentration diminishes the availability of free amino groups of CS due to crosslinking and leads to decrease in mucoadhesion of microspheres.

5.2.3.2.1.5. *Optimization of microspheres*

The final optimized formulation was produced based on combined effect of all the variables. The optimization of microspheres was obtained with the composite desirability of one by fixing targets for independent variables (Table 5.21). The optimized batch obtained at following conditions: CS (2.62%), VC (5.52%), and SC (2.22%). The predicted values of independent variables were validated with experimentally obtained values. The experimentally obtained values presented a sound agreement with acceptable percentage bias (< 15%). The outcome also justifies good fit of the model for predictions of results.

Table 5.21: Validation of optimized variables for microspheres

Factor	Optimized formulation	Desirability		
CS	2.62% w/v			
VAN	5.52% w/v	1		
SC	2.22% w/v			
Response	**Target Value**	**Predicted Value**	**Observed (mean± SD) (n = 3)**	**% Bias**
PS (µm)	< 50	49.95	46.88±1.25	6.15
EEOZ (%)	> 80	80.20	79.33±0.87	1.08
EEDX (%)	> 80	82.73	81.29±1.29	1.74
TDX (days)	> 7	8.29	8.77±.772	-5.75
TOZ (days)	> 7	7.73	7.85±.859	-1.42
% M	within range	67.53	75.45±5.45	-5.79

The final optimized CS-VAN microspheres were further incorporated into *in-situ* gel systems for feasibility of administration into periodontal pocket. The comparative aspects of characteristics of microspheres and microspheres loaded *in-situ* gel (MLIG) are discussed in next chapter 6.